Thesis for the Degree of Doctor of Philosophy in Natural Science, Specialization in Chemistry

Nitrogen-containing products from atmospheric oxidation of volatile organic compounds

Epameinondas Tsiligiannis

UNIVERSITY OF
GOTHENBURG

Department of Chemistry and Molecular Biology
Gothenburg, April 2022

Nitrogen-containing products from atmospheric oxidation of volatile organic compounds

Cover illustration: Anthropogenic and biogenic sources leading to formation of N-containing products, Luis Santos and Epameinondas Tsiligiannis.
Photo: Luis Santos and Epameinondas Tsiligiannis

ISBN 978-91-8009-723-9 (PRINT)
ISBN 978-91-8009-724-6 (PDF)

Department of Chemistry and Molecular Biology
University of Gothenburg
412 96 Gothenburg, Sweden

Printed by Stema AB
Borås, Sweden 2022

Abstract

Atmospheric oxidation of volatile organic compounds (VOC) produces a wide range of oxygenated organic products that lead to formation of secondary organic aerosol (SOA). SOA represents a significant fraction of the tropospheric aerosol that influence climate and human health. However, the level of understanding of SOA processes is low compared to other aerosol processes and one reason is the complexity of VOC oxidation under various conditions. VOC oxidation under high NO_x conditions or by nitrate radicals (NO_3) leads to formation of various nitrogen-containing compounds. The N-containing products, apart from contributing to SOA formation, can act as NO_x reservoir and/or as permanent sink affecting ozone formation. Also, organic nitrogen can play a role on the atmospheric nitrogen cycle, with ecological impacts.

In this work the focus is on the nitrogen-containing oxidation products in the gas phase and their contribution to the particle phase. Laboratory studies on OH-initiated oxidation of 1,3,5-trimethylbenzene (TMB) (an anthropogenic VOC) under different NO_x levels and NO3-initiated oxidation of isoprene (the most abundant non-methane biogenic VOC) were conducted utilizing the Go:PAM flow reactor and the atmospheric simulation chamber SAPHIR. The oxidation products from these reactions were detected using chemical ionization mass spectrometry. This method was also applied in the field to measure selected organonitrates related to the laboratory studies.

The TMB oxidation under elevated NO_x conditions favored the formation of organonitrates (ONs) reducing the amount of highly oxygenated organic molecules (HOM) monomers and especially the dimers, leading to suppression of new particle formation. Ambient observations of nitro-aromatic compounds originating from anthropogenic sources demonstrated that nitrophenol and its analogue can be used as direct tracers of primary emissions from biomass burning. NO_3 oxidation of isoprene produced monomers and dimers with 1 to 3 nitrate groups. The specifics of the various time evolutions indicating formation pathways from multi-generation secondary chemistry. Selected products from this secondary chemistry had high propensity to participate to the particle phase. Observations from six locations around the globe showed that the isoprene-derived ONs with chemical formula $C_4H_7NO_5$ observed in the laboratory did dominate the ambient gas phase product distribution both during nighttime and daytime.

To summarize, the objectives of this thesis are to advance our understanding on the nitrogen-containing products from atmospheric oxidation of different VOC, identify their reaction mechanisms and product distributions, and provide insights on their role to SOA formation.

Keywords: VOC, anthropogenic, biogenic, SOA, atmospheric oxidation, organic aerosols, CIMS, FIGAERO, TMB, isoprene, HOM, organonitrates (ONs), NO_x, OH, nitrate (NO_3), Go:PAM, SAPHIR

Sammanfattning

Atmosfärisk oxidation av flyktiga organiska föreningar (VOC) producerar ett brett utbud av syresatta organiska produkter som leder till bildning av sekundär organisk aerosol (SOA). SOA representerar en betydande del av den troposfäriska aerosolen som påverkar klimatet och människors hälsa. Men nivån av förståelse för SOA processer är låg jämfört med andra aerosolprocesser. VOC oxidation under höga NO_x-förhållanden eller av nitratradikaler (NO_3) leder till bildning av olika kvävehaltiga föreningar. De N-innehållande produkterna kan, förutom att bidra till SOA-bildning, fungera som NO_x-reservoar och/eller som permanent sänka som påverkar ozonbildningen. Organiskt kväve kan också spela en roll i atmosfärens kvävecykel, med ekologiska effekter.

I detta arbete ligger fokus på kväveinnehållande oxidationsprodukter i gasfas och deras eventuella bidrag till partikelfasen. Laboratoriestudier av OH-initierad oxidation av 1,3,5-trimetylbensen (TMB) (en antropogen VOC) under olika NO_x nivåer samt NO_3-initierad oxidation av isopren (den vanligaste biogena VOC) utfördes med hjälp av en oxidations flödesreaktor (Go:PAM) och den atmosfäriska simuleringskammaren SAPHIR. Oxidationsprodukterna detekterades med kemisk joniseringsmasspektrometri. Samma metod användas i fält för observation av utvalda organiska nitrater somvar relaterade till lab-studierna.

TMB oxidationen under förhöjda NO_x förhållanden gynnade bildningen av organonitrater (ON) på bekostnad av monomerer av mycket oxygenerade organiska molekyler (HOM) och till än högre grad av dimerer, vilket ledde till en minskad nypartikelbildning. Vid NO3 oxidationav isopren bildades monomer och dimerer med en till tre nitratgrupper. Observationerna i SAPHIR påvisade att flera av de kemiska bildningsvägarna omfattade flerstegsprocesser (sekundär kemi). Felar av de produkter som bildas via sekundär kemi hade hög benägenhet att bidra till partikelfasen. Mätningar av några av dessas produkter i utomhusluft från sex olika platser runt om i världenvisade att den ON med kemisk formel $C_4H_7NO_5$ dominerade både under natt och dag. Vid en annan fältmätningsstudie observerades nitroaromatiska föreningar som istället härrör från antropogena källor. Där identifieras nitrofenol och dess analoger vilket kunde användas för att uppskattat bidraget från primära utsläpp vid förbränning av biomassa.

Sammanfattningsvis var syftet med denna avhandling att främja vår förståelse av kväveinnehållande produkter från atmosfärisk oxidation av olika VOC, identifiera deras reaktionsmekanismer och produktfördelningar och få insikter om deras roll för SOA-bildning.

Nyckelord: VOC, anthropogen, biogen, SOA, atmosfärik oxidation, organisks aerosoler, CIMS, FIGAERO, TMB, isopren, HOM, organonitrater (ONs), NO_x, OH, nitrat (NO_3), Go:PAM, SAPHIR

Ιθάκη

Σα βγεις στον πηγαιμό για την Ιθάκη,
να εύχεσαι να 'ναι μακρύς ο δρόμος,
γεμάτος περιπέτειες, γεμάτος γνώσεις.
Τους Λαιστρυγόνας και τους Κύκλωπας,
τον θυμωμένο Ποσειδώνα μη φοβάσαι,
τέτοια στον δρόμο σου ποτέ σου δεν θα βρεις,
αν μέν' η σκέψις σου υψηλή, αν εκλεκτή
συγκίνησις το πνεύμα και το σώμα σου αγγίζει.
Τους Λαιστρυγόνας και τους Κύκλωπας,
τον άγριο Ποσειδώνα δεν θα συναντήσεις,
αν δεν τους κουβανείς μες στην ψυχή σου,
αν η ψυχή σου δεν τους στήνει εμπρός σου.

Να εύχεσαι να 'ναι μακρύς ο δρόμος.
Πολλά τα καλοκαιρινά πρωιά να είναι
που με τί ευχαρίστησι, με τί χαρά
θα μπαίνεις σε λιμένας πρωτοϊδωμένους
να σταματήσεις σ' εμπορεία Φοινικικά,
και τες καλές πραγμάτειες ν' αποκτήσεις,
σεντέφια και κοράλλια, κεχριμπάρια κι
έβενους,
και ηδονικά μυρωδικά κάθε λογής,
όσο μπορείς πιο άφθονα ηδονικά μυρωδικά
σε πόλεις Αιγυπτιακές πολλές να πας,
να μάθεις και να μάθεις απ' τους
σπουδασμένους.

Πάντα στον νου σου να 'χεις την Ιθάκη.
Το φθάσιμον εκεί είν' ο προορισμός σου.
Αλλά μη βιάζεις το ταξίδι διόλου.
Καλύτερα χρόνια πολλά να διαρκέσει·
και γέρος πια ν' αράξεις στο νησί,
πλούσιος με όσα κέρδισες στον δρόμο,
μη προσδοκώντας πλούτη να σε δώσει η
Ιθάκη.

Η Ιθάκη σ' έδωσε τ' ωραίο ταξίδι.
Χωρίς αυτήν δεν θα 'βγαινες στον δρόμο.
Άλλα δεν έχει να σε δώσει πια.

Κι αν πτωχική την βρεις, η Ιθάκη δεν σε
γέλασε.
Έτσι σοφός που έγινες, με τόση πείρα,
ήδη θα το κατάλαβες οι Ιθάκες τί σημαίνουν.

Κωνσταντίνος Καβάφης, περιοδικό Γράμματα, 1911

Ithaka

As you set out for Ithaka
hope your road is a long one,
full of adventure, full of discovery.
Laistrygonians, Cyclops,
angry Poseidon—don't be afraid of them:
you'll never find things like that on your way
as long as you keep your thoughts raised high,
as long as a rare excitement
stirs your spirit and your body.
Laistrygonians, Cyclops,
wild Poseidon—you won't encounter them
unless you bring them along inside your soul,
unless your soul sets them up in front of you.

Hope your road is a long one.
May there be many summer mornings when,
with what pleasure, what joy,
you enter harbors you're seeing for the first
time;
may you stop at Phoenician trading stations
to buy fine things,
mother of pearl and coral, amber and ebony,
sensual perfume of every kind—
as many sensual perfumes as you can;
and may you visit many Egyptian cities
to learn and go on learning from their
scholars.

Keep Ithaka always in your mind.
Arriving there is what you're destined for.
But don't hurry the journey at all.
Better if it lasts for years,
so you're old by the time you reach the island,
wealthy with all you've gained on the way,
not expecting Ithaka to make you rich.

Ithaka gave you the marvelous journey.
Without her you wouldn't have set out.
She has nothing left to give you now.

And if you find her poor, Ithaka won't have
fooled you.
Wise as you will have become, so full of
experience,
you'll have understood by then what these
Ithakas mean.

List of Papers

Publications included in this thesis:

I **Effect of NO_x on 1,3,5-trimethylbenzene (TMB) oxidation product distribution and particle formation.**
Tsiligiannis, E., Hammes, J., Salvador, C. M., Mentel, T. F., and Hallquist, M.: Atmos. Chem. Phys., 19, 15073-15086, 10.5194/acp-19-15073-2019, 2019

II **Ambient nitro-aromatic compounds – biomass burning versus secondary formation in rural China.** Salvador, C. M. G., Tang, R., Priestley, M., Li, L., **Tsiligiannis, E.**, Le Breton, M., Zhu, W., Zeng, L., Wang, H., Yu, Y., Hu, M., Guo, S., and Hallquist, M.: Atmos. Chem. Phys., 21, 1389-1406, 10.5194/acp-21-1389-2021, 2021.

III **Molecular composition and volatility of multi-generation products formed from isoprene oxidation by nitrate radical.** Wu, R., Vereecken, L., **Tsiligiannis, E.** Kang, S., Albrecht, S. R., Hantschke, L., Zhao, D., Novelli, A., Fuchs, H., Tillmann, R., Hohaus, T., Carlsson, P. T. M., Shenolikar, J., Bernard, F., Crowley, J. N., Fry, J. L., Brownwood, B., Thornton, J. A., Brown, S. S., Kiendler-Scharr, A., Wahner, A., Hallquist, M., and Mentel, T. F.: Atmos. Chem. Phys., 21, 10799-10824, 10.5194/acp-21-10799-2021, 2021.

IV **Gas-Particle Partitioning and SOA Yields of Organonitrate Products from NO_3-Initiated Oxidation of Isoprene under Varied Chemical Regimes.** Brownwood, B., Turdziladze, A., Hohaus, T., Wu, R., Mentel, T. F., Carlsson, P. T. M., **Tsiligiannis, E**, Hallquist, M., Andres, S., Hantschke, L., Reimer, D., Rohrer, F., Tillmann, R., Winter, B., Liebmann, J., Brown, S. S., Kiendler-Scharr, A., Novelli, A., Fuchs, H., and Fry, J. L.: ACS Earth and Space Chemistry, 10.1021/acsearthspacechem.0c00311, 2021.

V **A four carbon organonitrate as a significant product of secondary isoprene chemistry. Tsiligiannis, E.**, Wu, R., Lee, B. H., Salvador, C. M. G., Priestley, M., Carlsson, P. T.M., Kang, S., Novelli, A., Vereecken, L., Fuchs, H., Mayhew, A. W., Hamilton, J. F., Edwards, P. M., Fry, J. L., Brownwood, B., Brown, S. S., Wild, R. J., Bannan, T. J., Coe, H., Allan, J., Surratt, J. D., Bacak, A., Artaxo, P., Percival, C., Guo, S., Hu, M., Wang, T., Mentel, T. F., Thornton, J. A., and Hallquist, M., Under review to Geophysical Research Letters (2022).

Contribution report

I Epameinondas Tsiligiannis (ET) participated in the design of the experiments. ET performed the experiments and data analysis together with Julia Hammes (JH). ET performed the modeling. ET, JH and Mattias Hallquist (MH) wrote the paper.

II ET participated in the calibration procedures and the discussion on modeling/simulation experiments.

III ET participated in the NO_3ISOP campaign presented in the paper III. ET operated instrumentation and performed data analysis. ET participated in the interpretation of the compiled data set and the discussions on the results and commented the paper.

IV ET participated in the NO_3ISOP campaign presented in the paper IV. ET operated instrumentation and performed data analysis. ET contributed with Figures 7 & 10 and discussions and comments on the paper.

V ET participated in the conceptualization of the paper. ET participated in the NO_3ISOP and JULIAC campaigns presented in the paper V. ET operated instrumentation and performed data analysis. ET compiled the different data sets and interpreted them with the help of co-authors. ET wrote the paper under the supervision of MH.

Contents

List of Figures

List of Tables

List of Acronyms

2D-VBS	Two-Dimensional Volatility Basis Set
HO_2	Hydroperoxy radical
N_2O_5	Dinitrogen pentoxide
NO_2	Nitrogen Dioxide
NO_3	Nitrate radical
O_3	Ozone
RO_2	Peroxy radical
ABS	Ammonium Bisulfate
ANs	Alkyl Nitrates
API	Atmospheric Pressure Interface
AS	Ammonium Sulfate
AVOCs	Anthropogenic Volatile Organic Compounds
BB	BiomassBurning
Br-CIMS	Bromide Chemical Ionization Mass Spectrometer
BrC	Brown Carbon
BSQ	Big Segmented Quadrupole
BVOCs	Biogenic Volatile Organic Compounds
CCN	Cloud Condensation Nuclei
CI	Chemical Ionization
CPC	Condensation Particle Counter
DMS	Dimethyl Sulfide
DNP	Dinitrophenol
EEA	European Environment Agency

EI	Electron Impact
ELVOC	Extremely Low Volatility Organic Compounds
ESI	Electrospray Ionization
FIGAERO	Filter Inlet for Gases and AEROsols
GHG	Greenhouse Gases
Go:PAM	Gothenburg Potential Aerosol Mass
HOM	Highly oxygenated Organic Molecules
I-CIMS	Iodide Chemical Ionization Mass Spectrometer
IMR	Ion Molecule Reaction Chamber
IPCC	Intergovernmental Panel on Climate Change
IVOC	Intermediate Volatility Organic Compounds
LOD	Limit of Detection
LVOC	Low Volatility Organic Compounds
MCM	Master Chemical Mechanism
MCP	Micro-channel Plates
NAC	Nitro-aromatic Compounds
NB	Nitrobenzoic acid
NC	Nitrocatechol
NO	Nitric Oxide
NO_x	Nitrogen Oxides
NP	Nitrophenol
NPF	New Particle Formation
OFR	Oxidation Flow Reactor
OH	Hydroxyl radical
ONs	Organonitrates

OS_C	Carbon Oxidation State
OVOCs	Oxygenated Volatile Organic Compounds
PAHs	Polycyclic Aromatic Hydrocarbons
PAM	Potential Aerosol Mass
PAN	Peroxyacyl Nitrate
PB	Primary Beam
PFHA	Perfluorinated Heptanoic Acid $C_7HF_{13}O_2$
PFPA	Perfluorinated Pentanoic Acid $C_5HF_9O_2$
PTFE	Polytetrafluoroethylene
R	alkyl radical
RH	Relative Humidity
RO	Alkoxy radical
SAPHIR	Simulation of Atmospheric Photochemistry In a large Reactor chamber
SMPS	Scanning Mobility Particle Sizer
SOA	Secondary Organic Aerosol
SSQ	Short Segmented Quadrupole
SVOC	Semi-volatile Organic Compounds
TD-CRDS	Thermal Dissociation Cavity Ring-Down Spectrometer
TMB	1,3,5-trimethylbenzene C_9H_{12}
ToF	Time-of-Flight
ToF-CIMS	Time-of-Flight Chemical Ionization Mass Spectrometer
VOCs	Volatile Organic Compounds
VS	Voltage Scanning

Part I

Extended Summary

1

Introduction

Contents

1.1 The atmosphere

Earth's atmosphere is crucial for life on the planet as we know it. The atmosphere's composition has been evolved since Earth's birth, about 4.6 billion years ago. Earth's atmosphere is consisted primarily of the gases N_2 (~78%), O_2 (~21%) and Ar (~1%), and their concentrations are controlled over geologic timescales. Water vapor is found mainly in the lower atmosphere and its concentration varies depending on the meteorological conditions, reaching values up to 3%. The rest of the constituents are called trace gases and they represent less than 1%. However, the trace gases affect greatly atmosphere's chemistry and Earth's radiative balance (Seinfeld and Pandis, 2016).

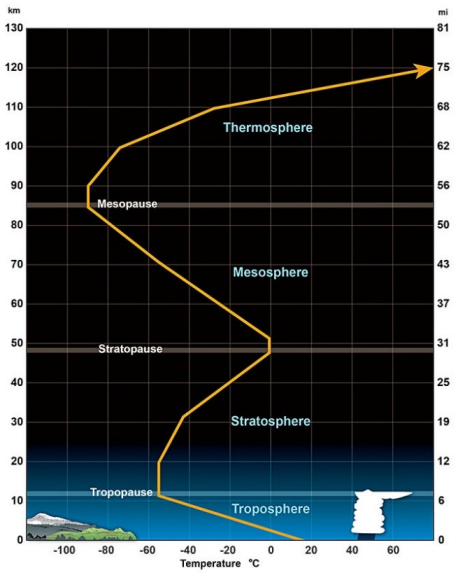

Figure 1.1: Average temperature profile for the lower layers of the atmosphere. Image credit: weather.gov, NOAA

The Earth's atmosphere is a complex system compromising a set of layers (figure 1.1), which differ in concentration, pressure, and temperature gradient with respect to altitude. The rate of temperature change in the atmosphere as a function of height can be used to define regions of negative or positive gradient. The first layer is called troposphere and the temperature decreases with height almost linearly up to the region known as tropopause. The troposphere extends up to 10 – 15 km altitude depending on the location and the time of the year. It can also be divided into the planetary boundary layer, from Earth's surface up to 1 km, and the free troposphere, from 1 km to the tropopause. The negative temperature gradient makes troposphere a very well-mixed layer, where most of the planet's weather takes place. Furthermore, most of atmosphere's water vapors and subsequently clouds are found in this layer. Troposphere contains about 80 - 90% of the atmosphere's mass and most of the reactive constituents, making it the main layer of focus in atmospheric chemistry.

The next layer is called stratosphere and extends from tropopause up to 45 – 50 km. At the tropopause a temperature inversion occurs, and the temperature increases with altitude mainly due to the absorption of solar radiation between 200 – 300 nm by the stratospheric ozone layer. The ozone layer is important for life on Earth as it absorbs harmful solar ultraviolet radiation. The observations of the ozone hole in the 1980's (Farman et al., 1985) demonstrated the ability of trace species to greatly influence atmosphere's chemistry. Stratosphere together with troposphere contain over 95% of atmosphere's mass.

Atmosphere's middle layer is mesosphere extending from stratopause to the mesopause, around 80 – 90 km. Here the temperature starts decreasing again, reaching the lowest values of the atmosphere. The upper atmosphere is called thermosphere and extends from mesopause up to 500 – 600 km altitude. A related mechanism as in the stratosphere results in a temperature increase. In this layer the absorption of short wavelength solar radiation, typically below 200 nm, by molecules, atoms, and ions is responsible for the increase, while the temperature of the thermosphere is modulated strongly by the solar cycle. The Aurora phenomenon takes place in the lower thermosphere. The final and outermost layer of the atmosphere is exosphere. The exosphere extends up to 10000 km where gas molecules with sufficient energy can escape into space.

1.2 Air pollution and climate change

The composition of the atmosphere as well as the concentrations of trace species are influenced by emissions originating from biogenic and/or anthropogenic sources. These emissions can interact with other gaseous molecules or airborne particles, undergoing chemical and physical transformation. Atmospheric constituents with adverse health effects are regarded as the cause of air pollution. The major atmospheric pollutants for human health are the nitrogen oxides (NO_x), tropospheric ozone (O_3), and particulate matter.

Nitric oxide (NO) and nitrogen dioxide (NO_2) are referred together as NO_x and are emitted by combustion engines or they are produced naturally by lighting. Tropospheric ozone, known also as ground-level ozone, is produced through the photochemical degradation of carbon monoxide and volatile organic compounds

(VOC) in the presence of NO_2 (Finlayson-Pitts and Pitts, 1999). Compared to the

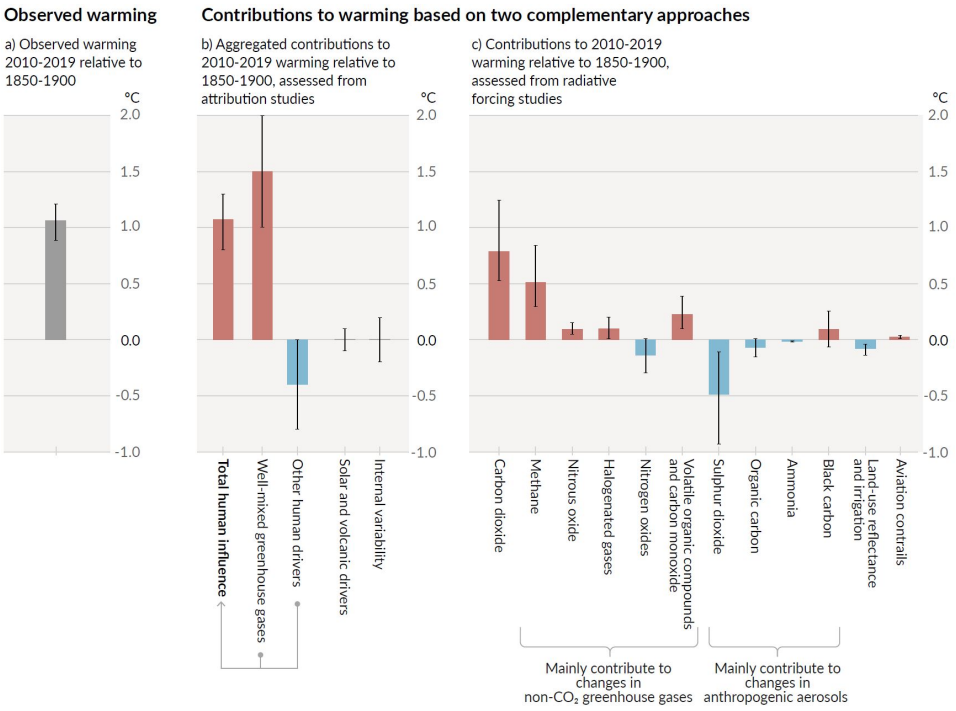

Figure 1.2: Assessed contributions to observed warming in 2010-2019 relative to 1850-1900. Panel a) Observed global warming. Panel b) Evidence from attribution studies. Panel c) Evidence from the assessment of radiative forcing and climate sensitivity. Reproduced from (Arias et al., 2021).

stratospheric ozone, which is essential for life on Earth, tropospheric ozone has direct harmful effects on humans by inhaling it and indirect by being a major component of photochemical smog. Aerosols are ubiquitous component of the atmosphere, and they are defined as a suspension of fine solid or liquid particles in a gaseous medium (atmospheric air). Particles are emitted directly to the atmosphere (primary aerosol) from natural sources, like sea spray, windborne dust, wildfires, and volcanoes, as well ae from human activities, such as combustion of fuels. They can also form in the atmosphere from gas-to-particle conversion (secondary aerosol) of vapor precursors. Aerosol composition consists of sulfate, ammonium, nitrate, sodium, chloride, carbonaceous material, trace metal and water (Seinfeld and Pandis, 2016). Particle size ranges from about 1 nm to 100 µm in diameter (Hinds, 1999).

Elevated particle concentration has been identified to have major implications in human health (Dockery et al., 1993; Fowler et al., 2020) causing cardiovascular and respiratory diseases (Dockery and Pope, 1994; Lelieveld et al., 2015). The European Environment Agency (EEA) has estimated 307000 premature deaths due to chronic exposure to fine particulate matter, 40400 premature deaths due to chronic NO_x exposure and 16800 premature deaths due to acute ozone exposure in European Union for the year 2019 (*Air quality in Europe 2021* 2022). Globally, exposure to air pollution is estimated to cause 7 to 8.8 million premature deaths every year and result in the loss of millions more healthy years of life (World Health, 2016; Lelieveld et al., 2019). Recently, aerosols gained more attention regarding their ability to carry viruses and bacteria, making them also relevant in disease transmission (Alsved et al., 2019; Tang et al., 2021) . Lastly, air pollution can also cause adverse effects on ecosystems, by creating and enhancing eutrophication and acidification (Fowler et al., 2020).

The atmospheric trace species also affect Earth's radiative balance. The greenhouse gases (GHG), such as carbon dioxide, methane, nitrous oxide, and halogenated compounds have a warming effect on the climate. Tropospheric ozone, apart from the harmful health effects, contributes also to warming climate. Aerosol particles depending on their composition and physicochemical properties can influence the radiative balance directly by scattering or absorbing solar radiation or indirectly by acting as cloud condensation nuclei (CCN) changing cloud properties (Fuzzi et al., 2015). Atmospheric particles provide surface, enabling heterogeneous condensation of water vapors, and subsequently the formation of clouds and rain. Without particles Earth's atmosphere would have been very different. In the latest report of Intergovernmental Panel on Climate Change (IPCC) the observed warming is attributed to emissions from human activities, with greenhouse gas warming partly masked by aerosol cooling (figure 1.2). The quantified effect of particles on climate still contains high uncertainties, making the study of their emissions, physical and chemical properties, and formation processes and their precursors highly necessary. Both air pollution and climate change are challenging issues of our era that need attention, actions and solutions and can be considered the two sides of the coin.

1.3 Thesis motivation and outline

A major component of the fine tropospheric aerosol, ranging from 20 up to 90%, is secondary organic aerosol (SOA) (Kanakidou et al., 2005; Kroll and Seinfeld, 2008; Jimenez et al., 2009; Li et al., 2018). SOA are formed in the atmosphere by gas-particle conversion processes such as new particle formation (NPF), condensation and heterogeneous and multiphase chemistry (Hallquist et al., 2009). Chemical degradation of volatile organic compounds (VOCs) is the major contributor to SOA. Despite their importance the current level of understanding of SOA processes is still remarkably low compared to other processes in aerosol science. In most climate models, the sources of SOA are treated in a very simplified way (Tsigaridis et al., 2014; Shrivastava et al., 2017), leading to large uncertainties. A recent study by (Sporre et al., 2020) showed that different treatment of natural-derived precursors of SOA in different models, results in large discrepancies in the direct and indirect aerosol radiative effect.

VOC oxidation produces a wide range of products with different functionalities and volatilities. Oxidation products with low enough volatility can contribute to NPF or growth of existing particles. Organic compounds such as carboxylic acids (Hammes et al., 2019; Glasius et al., 2021; Lutz et al., 2019), nitrates (Lee et al., 2016; Ng et al., 2017; Faxon et al., 2018; Hamilton et al., 2021), nitro-aromatics (Salvador et al., 2021), dimer esters (Kristensen et al., 2016; Mohr et al., 2017), epoxides (D'Ambro et al., 2019) have been identified to contribute to SOA formation. A new subgroup of organic vapors, highly oxygenated organic molecules (HOM), was first identified in laboratory studies and observed in a boreal forest area (Ehn et al., 2012; Ehn et al., 2014). HOM gained rapidly attention within the atmospheric science community, as most of these products characterized by low to extremely low saturation vapor pressures, contributing significantly to SOA (Bianchi et al., 2019). When VOCs react under high NO_x conditions or oxidized by nitrate radicals (NO_3), they form various nitrogen-containing compounds (Finlayson-Pitts and Pitts, 1999) . The N-containing products can act as NO_x reservoir and/or as permanent sink (Kiendler-Scharr et al., 2016), can affect ozone formation (Paulot et al., 2012; Schwantes et al., 2020), and can contribute to SOA formation (Lee et al., 2016). Furthermore, organic nitrogen can be a significant component of the atmospheric nitrogen cycle, with ecological impacts (Jickells et al., 2013). All in all, the N-containing compounds derived from VOC oxidation represent the human influence on atmospheric oxidation processes as NO_x or NO_3 radicals, both mainly

originate from anthropogenic sources, are necessary for their formation.

This thesis presents laboratory studies on the oxidation of 1,3,5-trimethylbenzene (TMB) and isoprene, using state-of-the-art instrumentation. Additionally, ambient observations of oxidation products from anthropogenic precursors and isoprene were used in order to create a more holistic picture. The objective of this thesis is to advance our understanding on the nitrogen-containing products from atmospheric oxidation of different VOC, identify their reaction mechanisms and product distributions, and provide insights on their role to SOA formation. More specifically the aim is to answer the following questions:

- How does NO_x influence the oxidation product distribution of TMB and particle formation? **(Paper I)**
- Which examples of nitrogen-containing compounds from human activities can be found in ambient atmosphere? **(Paper II)**
- What are the nighttime oxidation products of isoprene and how their yield change under different chemical conditions? **(Paper III and Paper IV)**
- What do ambient observations of isoprene nitrates tell us? **(Paper V)**
- How the mass loading and the acidity affect the partitioning of nighttime oxidation organonitrate products of isoprene?

The thesis has two parts: an extended summary and the attached papers. The first part consists of six chapters. Chapter 1 outlines a general introduction to the atmosphere, air pollution and climate change as well as the thesis motivation and outline. Chapter 2 provides more detailed background on tropospheric chemistry and SOA formation. Chapter 3 describes the instrumentation, laboratory reactors and methods that have been used within this thesis. A summary of the results and the key findings are discussed in Chapter 4 answering in parallel the aforementioned questions. Concluding remarks and their atmospheric implications are described in Chapter 5. Finally, Chapter 6 briefly presents ideas for future work.

Five papers are included in the second part. The first two papers are focusing on oxidation products containing nitrogen of VOCs from human sources whilst paper III-VI focus on nitrogen-containing products from isoprene, i.e. the dominant VOC from natural sources. Paper I focuses on the oxidation of TMB by OH radicals and the effects of NO_x on HOM and organonitrate (ON) formation, while the observed suppression of NPF is linked to the product distribution. Ambient

measurements of nitro-aromatic compounds from anthropogenic activities in rural China are presented in Paper II. Paper III discusses the oxidation products of isoprene by nitrate radical, providing a mechanistic pattern analysis and insights of their volatilities. Paper IV deals with the bulk alkyl nitrates and SOA yields from the NO_3-initiated oxidation of isoprene. Paper V combines laboratory experiments, ambient data, and modeling to investigate major secondary organonitrates from isoprene oxidation.

2

Tropospheric Chemistry and Aerosol Formation

Contents

This chapter introduces the volatile organic compound, their basic tropospheric chemistry pathways depending on different conditions as well as their oxidation products and their connection to secondary organic aerosol formation.

2.1 Volatile Organic Compounds

Volatile Organic Compounds (VOCs) are gases emitted from both natural and human sources into the atmosphere. A total amount of about 1200 – 1300 Tg C yr^{-1} has been estimated to be emitted (Jickells et al., 2013; Glasius and Goldstein, 2016).

Biogenic VOC (BVOC) are emitted from natural sources and their contribution to the total VOC is estimated around 75 – 90% (Guenther et al., 1995). Half of the non-methane BVOC emissions consist of isoprene, followed by monoterpenes 15% and sesquiterpenes 3% (Carlton et al., 2009; Guenther et al., 2012). Other compounds with a somewhat high contribution are methanol, ethanol, acetaldehyde, acetone, ethene, and propene (Guenther et al., 2012). Flowers emit VOCs to attract pollinators (Schiestl, 2010), while plants emissions are induced by biotic or abiotic stresses such as attacks by herbivores or pathogens, drought or high temperatures, and generally oxidative stress (Sharkey et al., 2007; Loreto et al., 2014). Groups of plants emit different VOCs, for example tropical forest are dominated by isoprene emissions (Müller et al., 2008), whilst monoterpenes such as α-pinene dominate boreal forests (Hakola et al., 2012).

Isoprene (2-methyl-1,3-butadiene, C_5H_8) chemistry significantly affects tropospheric ozone (Schwantes et al., 2020) and the rate of oxidation of other VOCs by perturbating NO_x and HO_x cycles (Peeters et al., 2009). Due to its abundance isoprene can contribute significantly to global SOA mass even if it has low SOA yields (Kroll et al., 2005; Kleindienst et al., 2007; Brownwood et al., 2021; Carlton et al., 2009) while recent studies have shown that it can also reduce SOA in mixture of atmospheric VOCs (McFiggans et al., 2019; Heinritzi et al., 2020). Because of its double bonds, isoprene is highly reactive in the atmosphere.

In urban areas, a significant part of the emissions consists of anthropogenic VOC (AVOC). They are emitted by human activities such as transportation, indus-

trial processes, solvent use, biomass burning, fuel combustion, and cosmetics and personal-care products (McDonald et al., 2018) and their emissions are mainly dominated by aromatics, alkanes, and alkenes (Li et al., 2019a). The dominant aromatics in the atmosphere are benzene, toluene, ethylbenzene, xylenes, styrene, and trimethylbenzenes.

Many studies on aromatics oxidation have shown that they have high SOA yields (Ng et al., 2007; Wyche et al., 2009; Gentner et al., 2017; Li et al., 2021). Furthermore, aromatics may play a role in ozone formation in heavy-polluted areas (Porter et al., 2017). However, the representation of gas-phase aromatics chemistry and SOA formation have been either neglected or highly simplified in global atmospheric models (Henze et al., 2008; Cabrera-Perez et al., 2016; Taraborrelli et al., 2021; Bates et al., 2021) . Despite the lower emissions of AVOCs compared to BVOCs, their emissions and oxidation products can be of high importance for human health. Enhanced emissions of polycyclic aromatic hydrocarbons (PAHs), long known for their mutagenic and carcinogenic effects, linked to domestic biomass burning increasing the PAHs exposure and cancer risk (Tsiodra et al., 2021). Also, SOA formed from AVOC may be responsible for high oxidative potential concentrations (Daellenbach et al., 2020) and higher air pollution mortality (Nault et al., 2021).

2.2 Atmospheric oxidants

Gas-phase oxidation is the primary process for transformation and loss of volatile organic compounds. The oxidation is initiated by reaction with atmospheric oxidants like the hydroxyl radical (OH), ozone (O_3), nitrate radical (NO_3) or via photolysis, (Kroll and Seinfeld, 2008).

The primary oxidizing species in the troposphere is the OH radical. OH concentrations are much more significant during daytime compared to night (table 2.1). OH reacts with almost everything very fast, having a lifetime of a few seconds (Seinfeld and Pandis, 2016). Aromatics, such as TMB, and isoprene react quite fast with OH radicals with a lifetime of a few minutes (table 2.2). OH concentrations range from $1 - 10 \times 10^6$ molecules cm^{-3} (Finlayson-Pitts and Pitts, 1999) with the highest values in the tropics and during summer (Lelieveld et al., 2016).

Table 2.1: Average oxidant mixing ratios and concentrations for polluted urban environments. Adapted from (Calvert et al., 2002).

Oxidant	Daytime average		Nighttime average	
	Volume mixing ratio	molecules cm^{-3}	Volume mixing ratio	molecules cm^{-3}
OH	0.16 pptv	$3.9x10^6$	0.0007 pptv	$1.4x10^4$
O_3	110 ppbv	$2.7x10^{12}$	80 ppbv	$2.0x10^{12}$
NO_3	3 pptv	$7x10^7$	100 pptv	$2.5x10^9$

In general, O_3 has lower reaction rates compared to OH radicals but its high concentrations making it an important oxidant, especially to unsaturated compounds. The elevated concentrations during nighttime, compared to OH, make O_3 an important oxidant throughout the day. The global mean lifetime of an ozone molecule are estimated to be 19 days (Seinfeld and Pandis, 2016). A double bond is needed in order to initiate oxidation by O_3, thus isoprene reacts with O_3 relatively quick. On the other hand, the ozonolysis of aromatics is very slow (table 2.2).

NO_3 radicals are photolyzed rapidly during daytime making the NO_3-initiated oxidation unimportant during daytime. However, under dense clouds or forest canopies NO_3 chemistry may still be important during daytime (Wennberg et al., 2018). Typical NO_3 mixing ratios in the nocturnal boundary layer range between 10 to 100 ppt (Seinfeld and Pandis, 2016), although values of a few hundred ppt have been measured (Brown and Stutz, 2012). The reaction rate of NO_3 with isoprene is quite fast while its reaction with TMB much slower compared to OH but faster compared to ozonolysis (table 2.2).

2.2.1 OH

OH primary formation pathway is the photodissociation of ozone followed by reaction with water vapor. The produced excited oxygen, $O(^1D)$, mainly collides with another molecule, M, returning to its ground state $O(^3P)$, while a minority of

Table 2.2: Atmospheric lifetimes for TMB and isoprene for their reaction with OH radicals, ozone, and NO_3 radicals.

	OH	O_3	NO_3
compound	12 hrs daytime[a]	24 hours[a]	12 hrs nighttime [a]
TMB [b]	2.4 h	20.5 years	52 days
Isoprene [c]	1.4 h	1.3 day	1.6 h

[a] average concentrations [molecules cm^{-3}]: 2 x 10^6 OH, 7 x 10^{11} O_3, and 2.5 x 10^8 NO_3 (Atkinson and Arey, 2003), [b] k_{TMB}+OH = 5.7 x 10^{-11}, k_{TMB} + O_3 = 2.2 x 10^{-21}, k_{TMB} + NO_3 = 8.8 x 10^{-16}, (Calvert et al., 2002), [c] $k_{Isoprene+OH}$ = 1.0 x 10^{-10}, $k_{Isoprene+O_3}$ = 1.3 x 10^{-17}, $k_{Isoprene+NO_3}$ = 7.0 x 10^{-13} (Atkinson et al., 2006). All reaction rates in cm^3 $molecules^{-1}$ s^{-1} at T = 298 K.

$O(^1D)$ reacts with water vapors to form OH (Lelieveld et al., 2016).

$$O_3 + hv(\lambda \leq 330nm) \longrightarrow O(^1D) + O_2 \quad (C\,2.1)$$

$$O(^1D) + M \longrightarrow O(^3P) + M \quad (C\,2.2)$$

$$O(^1D) + H_2O \longrightarrow 2OH \quad (C\,2.3)$$

In urban polluted areas OH formation includes the photolysis of nitrous oxide, HONO, and hydrogen peroxide, H_2O_2 (Fu et al., 2019).

$$HONO + hv(\lambda \leq 400nm) \longrightarrow OH + NO \quad (C\,2.4)$$

$$H_2O_2 + hv(\lambda \leq 550nm) \longrightarrow 2OH \quad (C\,2.5)$$

In air influenced by pollution OH formation is influenced by the NO_x recycling mechanism of OH, via the reaction of hydroperoxyl radicals, HO_2, with nitric oxide, NO (Lelieveld et al., 2016).

$$HO_2 + NO \longrightarrow OH + NO_2 \quad (C\,2.6)$$

Lastly, alkene ozonolysis can give OH radicals and be an important source during nighttime.

2.2.2 O_3

Tropospheric ozone formation occurs through the photolysis of NO_2, followed by the reaction of $O(^3P)$ with O_2. Close to fresh NO_x emissions O_3 can react with NO giving back NO_2. The oxidation of CO, methane, and VOCs by OH radicals under high NO_x conditions is feeding the ozone cycle. The relation between O_3, NO_x, and VOCs is not linear and detailed representation of the VOC oxidation is necessary to better estimate the O_3 levels (Schwantes et al., 2020).

$$NO_2 + h\nu(\lambda \leq 430nm) \longrightarrow NO + O(^3P) \quad (C\,2.7)$$

$$O(^3P) + O_2 + M \longrightarrow O_3 + M \quad (C\,2.8)$$

$$NO + O_3 \longrightarrow NO_2 + O_2 \quad (C\,2.9)$$

2.2.3 NO_3

NO_2 does not photolyze at night, and subsequently the NO_x chemistry is different at nighttime. NO reacts with O_3 forming NO_2, and as a result almost all NO_x is in the form of NO_2. The NO_2 molecules react with O_3 to give NO_3 radicals. The nitrate radicals photolyze rapidly during daytime, resulting in NO_2 or NO. Also, NO_3 reacts very fast with NO giving two NO_2 molecules.

$$NO_2 + O_3 \longrightarrow NO_3 + O_2 \quad (C\,2.10)$$

$$NO_3 + h\nu(\lambda \leq 580nm) \longrightarrow NO_2 + O \quad (C\,2.11)$$

$$NO_3 + h\nu(\lambda \leq 700nm) \longrightarrow NO + O_2 \quad (C\,2.12)$$

$$NO_3 + NO \longrightarrow 2\,NO_2 \quad (C\,2.13)$$

At night NO_3 can react with NO2 producing the thermally unstable N_2O_5. NO_3 and N_2O_5 exist in an equilibrium, while the N_2O_5 can be hydrolyzed on aerosol forming HNO_3 (Hallquist et al., 2000).

$$NO_3 + NO_2 + M \longrightarrow N_2O_5 + M \quad (C\,2.14)$$

$$N_2O_5 + H_2O(\text{surface}) \longrightarrow 2\,HNO_3(aq) \qquad (C\,2.15)$$

2.3 RO_2 and RO chemistry (Oxidation of VOC)

A general overview of the VOC degradation mechanism initiated by OH radicals is shown in figure 2.1. The oxidation starts with the formation of an alkyl radical (R), followed by rapid O_2 addition and the formation of peroxy radical (RO_2) and alkoxy radical (RO). Different termination pathways lead to different intermediates and products.

The VOCs studied within this thesis are isoprene and TMB. The OH-initiated oxidation of alkenes, like isoprene, proceeds mainly with the OH addition to the double bond forming an alkyl radical. In the NO_3-initiated oxidation of alkenes, NO_3 undergoes addition to the double bond in much the same way as OH (Finlayson-Pitts and Pitts, 1999) (figure 2.2). On the other hand, oxidation of aromatics by OH radicals can proceed either via a hydrogen abstraction or OH addition (figure 2.2). The fate of the formed peroxy radicals depends on chemical conditions (figure 2.1). Under low-NO_x conditions they react with HO_2, with other RO_2 or undergo intramolecular isomerization.

The formation of hydroperoxides (reaction C 2.16) is the primary pathway of the reaction of a peroxy radical with HO_2. For more complex RO_2 reactions with smaller contribution can also yield carbonyls and alcohols (reactions C 2.17 and C 2.18). Finally, this reaction can also generate alkoxy radicals (reaction C 2.19).

$$RO_2 + HO_2 \longrightarrow ROOH + O_2 \qquad (C\,2.16)$$

$$RO_2 + HO_2 \longrightarrow \text{carbonyl} + HO_2 + O_2 \qquad (C\,2.17)$$

$$RO_2 + HO_2 \longrightarrow ROH + O_3 \qquad (C\,2.18)$$

$$RO_2 + HO_2 \longrightarrow RO + OH + O_2 \qquad (C\,2.19)$$

The self-reaction of RO_2 or the cross reaction with a $RO_2{}'$ of different structure have three major channels. The formation of alkoxy radicals (RO) (reaction C 2.20), the formation of termination products such as alcohols and carbonyls (reaction

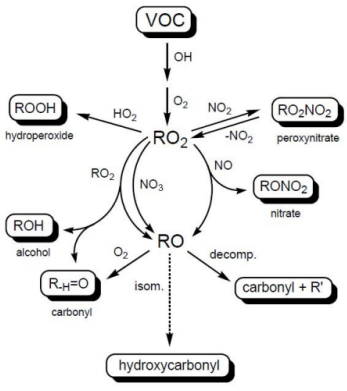

Figure 2.1: General oxidation mechanism of VOC by OH radicals. Reproduced from (Hallquist et al., 2009)

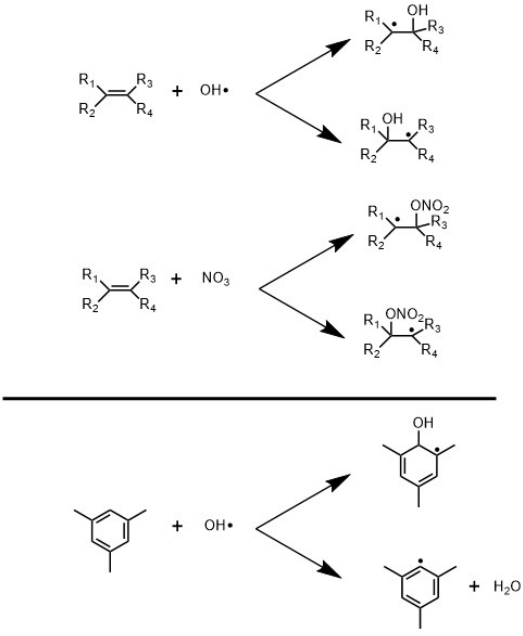

Figure 2.2: (top) OH and NO_3-initiated oxidation of and alkene by addition. (bottom) OH oxidation of an aromatic via OH addition or H abstraction.

C 2.21) as well as accretion products (reaction C 2.22). The latter has the lowest yield compared to other two, but it can significantly contribute to SOA formation (McFiggans et al., 2019).

$$\mathrm{RO_2 + RO_2 \longrightarrow 2\,RO + O_2} \tag{C 2.20}$$

$$\mathrm{RO_2 + RO_2 \longrightarrow ROH + RCHO + O_2} \tag{C 2.21}$$

$$\mathrm{RO_2 + RO_2 \longrightarrow ROOR + O_2} \tag{C 2.22}$$

Finally, intramolecular isomerization of larger RO_2 radicals is also possible if the RO_2 lifetime is long enough. This pathway will be discussed in the next section in conjunction with formation of highly oxygenated organic molecules (HOM). Alkoxy radicals (RO) have different atmospheric fates, depending on their particular structure (Finlayson-Pitts and Pitts, 1999). If there is a hydrogen at

the carbon in which is attached to the alkoxy oxygen, then it can react with O_2 giving a hydroperoxyl radical and a carbonyl (Reaction C 2.23). Fragmentation gives smaller carbon chains (Reaction C 2.24), and it is more important for RO with increasing number of oxygen-containing substituents (Vereecken and Peeters, 2009). Intramolecular isomerization by H-shift in RO leads to the formation of new and more oxidized peroxy radicals (Reaction C 2.25).

$$RO + O_2 \longrightarrow \text{carbonyl} + HO_2 \quad \text{(C 2.23)}$$

$$RO \longrightarrow R'{=}O + R'' \quad \text{(C 2.24)}$$

$$RO \longrightarrow HOQ;HOQ + O_2 \longrightarrow R(OH)O_2 \quad \text{(C 2.25)}$$

Finally, other reactions such as dissociation of peroxy radicals or epoxidation of alkyl radicals with a hydroperoxy functionality (–OOH) may be of importance, whereas oxidation pathways can be further influenced by the presence of NO_x and SO_2.

2.4 NO_x effect on RO_2 and RO chemistry

NO_x concentrations are elevated at anthropogenically influenced environments. NO_x levels have complex non-linear effects on SOA formation, affecting several factors such as RO_2 reactions, product distribution and aerosol volatility(Shrivastava et al., 2017).

In the presence of NO_x, the peroxy radicals react with NO leading to alkoxy radicals and NO_2 (Reaction C 2.26) (Ziemann and Atkinson, 2012). This reaction is quite fast and dominates over the other RO_2 pathways in polluted areas. It also plays a major role in ozone formation in the troposphere, as NO_2 is formed and through its photolysis, ozone is ultimately produced. For larger RO_2 radicals the reaction with NO can also lead to the generation of alky nitrates (or organonitrates, ONs) (Reaction C 2.27). Organonitrates can act as reservoirs of reactive nitrogen, influencing ozone and SOA formation. Lastly, peroxy radicals can react with NO_2 in a three-body reaction to form peroxynitrates (Reaction C 2.28). Peroxynitrates can thermally decompose back to RO_2 and NO_2 quite fast, whilst their decomposition lifetime is increasing significantly with lower temperatures, e.g. at higher altitudes

(Ziemann and Atkinson, 2012).

$$RO_2 + NO \longrightarrow RO + NO_2 \quad \text{(C 2.26)}$$

$$RO_2 + NO \longrightarrow RONO_2 \quad \text{(C 2.27)}$$

$$RO_2 + NO_2 \overset{M}{\longleftrightarrow} ROONO_2 \quad \text{(C 2.28)}$$

Under high NO_x conditions, alkoxy radicals may also react either with NO or NO_2 (Reactions C 2.29 and C 2.30). However, these reactions are less likely compared to Reactions C 2.23 – C 2.25.

$$RO + NO \xrightarrow{M} RONO \quad \text{(C 2.29)}$$

$$RO + NO_2 \xrightarrow{M} RONO_2 \quad \text{(C 2.30)}$$

The reaction of NO_2 with O_3 (Reaction C 2.10) leads to the formation of NO_3 radicals. This has two effects. Firstly, the majority of the produced RO_2 radicals from NO_3-initiated oxidation of unsaturated compounds will contain nitrogen (figure 2.2) and secondly, RO_2 can react with NO_3 radicals forming NO_2 and alkoxy radicals (Reaction C 2.31).

$$RO_2 + NO_3 \longrightarrow RO + NO_2 + O_2 \quad \text{(C 2.31)}$$

2.5 HOM formation

Highly oxygenated organic molecules (HOM) are gaseous compounds that can contribute significantly to SOA formation (Ehn et al., 2014).They formed from a series of reactions where an initial RO_2 radical undergoes intramolecular isomerization via H-shift and rapid O_2 addition. The oxidation propagates via subsequent intramolecular H-shifts and O_2 additions. This mechanism is called autoxidation (Crounse et al., 2013) and it was known as an important pathway for RO_2 radicals in high temperature combustion and food spoiling, but it was considered unimportant in atmospheric chemistry due to the high energy barriers for the initial steps (Barsanti et al., 2017). However, the presence of functional groups in larger RO_2 can lower these barriers, enabling H-shift reactions at tropospheric conditions.

The mechanism is schematically depicted in figure 2.3.

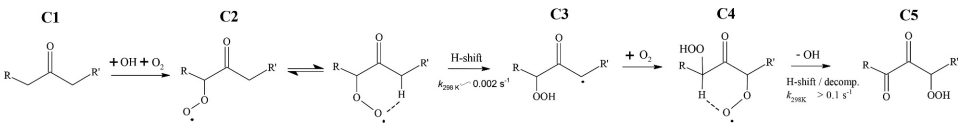

Figure 2.3: Autoxidation mechanism in OH-initiated oxidation of ketones. Reproduced from (Bianchi et al., 2019).

Specifically, the initial RO_2 internally abstracts a hydrogen from a carbon within the molecule forming an alkyl radical with a hydroperoxide functionality, followed by a rapid addition of O_2, and generation of a more oxidized RO_2. This process can be repeated creating even more oxidized RO_2 and leading to highly oxidized termination products.

HOM were initially considered having extremely low volatility due to the high number of oxygens (Ehn et al., 2014). However, later studies showed that they can also be low and even semi-volatile compounds (Kurtén et al., 2016; Tröstl et al., 2016). Three criteria have been suggested in a recent review on HOM by (Bianchi et al., 2019) in order to classify a molecule as a HOM. These are:

- HOM are formed via autoxidation involving peroxy radicals.
- HOM are formed in the gas phase, under atmospherically relevant conditions.
- HOM typically contain six or more oxygen atoms.

After the first observations and experiments on HOM formation (Ehn et al., 2010; Ehn et al., 2012) many studies have been conducted focusing on biogenic precursors and particularly on ozonolysis of α-pinene (Jokinen et al., 2015; Tröstl et al., 2016; Zhao et al., 2018; Molteni et al., 2019). Nevertheless, ozonolysis and OH-initiated oxidation (Jokinen et al., 2015; Berndt et al., 2016; Li et al., 2019b) as well as NO_3-initiated oxidation (Zhao et al., 2021) of different terpenes have also been studied. The role of HOM from biogenic precursors in mixtures has also been the focus of a few studies (Lehtipalo et al., 2018; McFiggans et al., 2019; Pullinen et al., 2020; Heinritzi et al., 2020).

Fewer studies on HOM formation originating from anthropogenic VOCs have been conducted compared to ones from BVOC precursors, however, AVOCs can also be a source of HOM (Rissanen, 2021). OH-initiated oxidation of aromatics leads to a

subsequently autoxidation chain reaction forming HOM (Wang et al., 2017; Molteni et al., 2018). Furthermore, the effect of NO_x emissions on different HOM AVOC precursors has been studied (Tsiligiannis et al., 2019; Garmash et al., 2020; Wang et al., 2020; Priestley et al., 2021).

Apart from the boreal forest (Ehn et al., 2014; Zha et al., 2018) HOM have also been detected in other areas. (Jokinen et al., 2014) and (Kürten et al., 2016) detected HOM in suburban and rural areas in Germany, respectively. HOM have been measured at a rural site in southeastern USA dominated by isoprene emissions (Krechmer et al., 2015; Lee et al., 2016; Massoli et al., 2018). In addition, HOM have been monitored in urban areas in China (Brean et al., 2019; Mehra et al., 2021; Xu et al., 2021). Finally, HOM formation have even been observed in the free troposphere (Bianchi et al., 2016; Frege et al., 2017).

The detailed degradation schemes of the most dominant VOCs by the main oxidants (OH, O_3 and NO_3) are used in different chemical mechanistic models. One of the most widely used mechanistic models is the master chemical mechanism (MCM). MCM represents in a near-explicit way both the degradation of non-aromatic (Saunders et al., 2003; Jenkin et al., 2015) and aromatic (Jenkin et al., 2003; Bloss et al., 2005) VOCs. MCM was developed with a primary goal to describe ozone formation while its explicit representation of reactions has made it an important tool on evaluation of laboratory chamber and flow reactor studies. However, the majority of highly oxidized gas-phase products that can contribute to SOA formation are not included in the MCM leading to an underprediction of SOA yields. Recent mechanistic development has started to take into account the autoxidation mechanism and HOM formation, based on HOM produced from α-pinene oxidation, in conjunction with MCM to improve the SOA mass yield estimation (Xavier et al., 2019).

2.6 Volatility, phase partitioning and SOA formation

The fate of atmospheric VOC oxidation products is to partition between gas and particle phase after further reactions or get removed from the atmosphere by wet or dry deposition. If the products remain in the gas phase or go to the particle phase, it depends on their vapor pressure. The vapor pressure of a molecule is determined

by its polarity, functional groups, and size (Kroll and Seinfeld, 2008). The pressure of a vapor in equilibrium with the condensed phase at a given temperature, i.e., when the number of molecules evaporating and condensing is equal, is defined as the saturation vapor pressure (Vehkamäki and Riipinen, 2012).

The gas-particle partitioning of organic species is the physical process that sets the distribution of a compound between the gas and particle phase. Partitioning is characterized by the saturation vapor pressure or equilibrium partitioning coefficient of molecules (Pankow, 1994). The partitioning coefficient,K_i, is given by the following formula:

$$K_i = \frac{[i]_{particle}}{[i]_{gas} * M_{org}} = \frac{RT}{\overline{MW_{om}}\gamma_i p_i^0} \tag{2.1}$$

where $[i]_{particle}$ and $[i]_{gas}$ are the concentrations of a compound i in the particle and gas phase, respectively, and M_{org} is the total aerosol organic mass. R is the gas constant and T the temperature; MW_{om} is the mean molecular mass of the particle components; γ_i is the activity coefficient, and p_i^0 is the saturation vapor pressure, p_s, of i. A key feature of partitioning theory is that the phase distribution depends on aerosol concentration (Donahue et al., 2009).

Volatility is a property of a compound that describes the tendency of it to exist as a vapor. The lower the saturation vapor pressure, the lower is the volatility of a compound. To describe progressive oxidation chemistry in a simplified but coherently way a classification framework, called two-dimensional volatility basis set (2D-VBS), based on two measurable organic properties, volatility and the degree of oxidation has been developed and widely used (Donahue et al., 2006; Donahue et al., 2011; Jimenez et al., 2009).

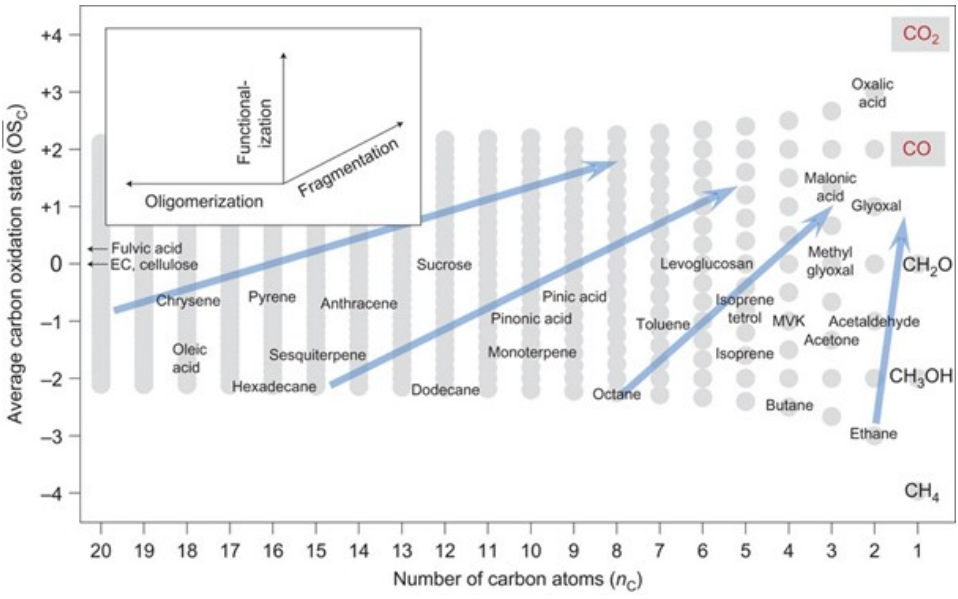

Figure 2.4: Diagram of average carbon oxidation state (OS_C) and number of carbon atoms (nC) for stable organic molecules, showing their oxidation evolution. Reproduced from (Kroll et al., 2011).

The extent of oxygenation (y-axis) has been expressed as O:C ratio in the initial model (Donahue et al., 2011), but the usage of the average oxidation state of carbon (OS_C) was quickly adapted as the principal y-axis (Donahue et al., 2012). The OS_C was preferred instead of O:C ratio because it is a parameter that always increases with oxidation, demonstrating the oxidation progress (Kroll et al., 2011). Initially, OS_C together with the organic carbon number (n_C) as the second dimension (figure 2.4) have been used in a different framework to describe the chemistry of atmospheric organic aerosol (Kroll et al., 2011).

The average oxidation state of carbon is determined by the identity and abundance of non-carbon atoms in the compound and defined as:

$$\overline{OS}_C = -\sum_i OS_i \frac{n_i}{n_C} \tag{2.2}$$

where OS_i the oxidation state of the element i, and $\frac{n_i}{n_C}$ is the molar ratio of element i to carbon. As atmospheric organics are primarily composed of carbon, hydrogen,

oxygen, and nitrogen, then the equation 2.2 can be simplified to:

$$\overline{OS}_C \approx 2(O:C) - (H:C) - 5(N:C) \tag{2.3}$$

The volatility (x-axis) in the 2D-VBS is expressed in terms of saturation mass concentration C^0 (µg m^{-3}), as mass concentration measurements are prevalent in atmospheric science, and it is proportional to saturation vapor pressure. C^0 is the saturation concentration of a vapor over a single component, while the saturation concentration over a mixture is given by the effective saturation concentration C*, including the activity coefficient, γ. C* is the inverse of partitioning coefficient, K_i, and can be expressed as:

$$\gamma * C^0 = C* = M_{org} * \frac{[i]_{gas}}{[i]_{particle}} \tag{2.4}$$

The 2D-VBS classifies the atmospheric compounds according to their volatility utilizing their effective saturation concentration, C*, expressed in µg m^{-3} in the following categories (Donahue et al., 2012):

- Extremely low volatility organic compounds (ELVOC, C*< 3 x 10^{-5} µg m^{-3}) which will condense irreversibly onto any pre-existing clusters and particles and may participate in NPF.
- Low volatility organic compounds (LVOC, 3 x 10^{-5} µg m^{-3} < C*< 0.3 µg m^{-3}) which will condense onto any sufficiently large particles and are predominantly in particle phase.
- Semi-volatile organic compounds (SVOC, 0.3 µg m^{-3} < C*< 300 µg m^{-3}) which exist in significant fractions in both particle and gas phases at equilibrium.
- Intermediate volatility organic compounds (IVOC, 300 µg m^{-3} < C*< 3 x 10^6 µg m^{-3}) which are almost exclusively in the gas-phase in the atmosphere.
- Volatile organic compounds (VOC, C*> 3 x 10^6 µg m^{-3}) which are gaseous compounds that dominate gas-phase oxidation chemistry in the atmosphere.

The range of volatilities of potential HOM products is given as an example (figure 2.5). HOM products fall mainly in ELVOC and LVOC classes with a smaller part in SVOC class. Due to this HOM may play a role in NPF (Tröstl et al., 2016) and SOA growth (Mohr et al., 2019).

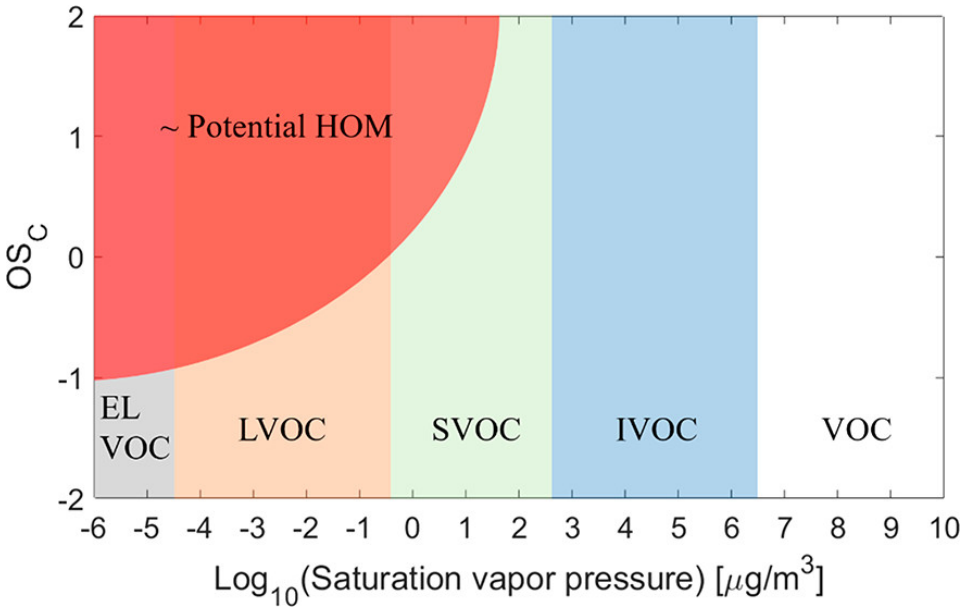

Figure 2.5: Potential HOM distribution in the 2D-VBS. Reproduced from (Bianchi et al., 2019).

To sum up, the major mechanism of SOA mass production is oxidation of gas-phase organic species and formation of vapors which partition in the particle phase (Riipinen et al., 2012). This mechanism proceeds through functionalization, oligomerization, and fragmentation. Oligomerization and functionalization can decrease the volatility and increase the water solubility of compounds by increasing the intramolecular forces between molecules, through addition of more polar oxygenated functional groups. Oligomerization is exhibiting strong NO_x dependence. On the other hand, fragmentation leads to products which tend to be more volatile (Hallquist et al., 2009).

This thesis is focusing on products from gas-phase chemistry of VOCs and their effects. Nevertheless, products from multi-phase chemistry, including heterogeneous and aqueous phase reactions, may be important for SOA formation and their properties (Pöschl and Shiraiwa, 2015; George et al., 2015) but our understanding is still limited.

3

Methodology

Contents

This chapter presents the key experimental tools and instrumentation used in this thesis, their abilities, and limitations to understand the complexity of atmospheric oxidation.

3.1 Go:PAM

The Potential Aerosol Mass (PAM) reactor is an oxidation flow reactor (OFR), which provides a highly oxidizing environment, enabling simulation of atmospheric oxidation processes of timescales ranging from one to several days, in a few minutes in the laboratory (Kang et al., 2007). The Gothenburg Potential Aerosol Mass (Go:PAM) reactor has been developed in the University of Gothenburg and was first described in the study by (Watne et al., 2018). Briefly, the Go:PAM consists

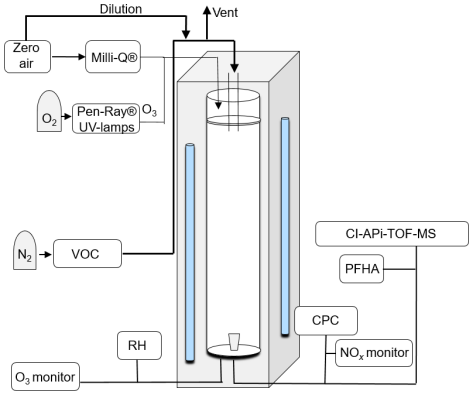

Figure 3.1: Schematic of the experimental setup using the Go:PAM flow reactor during the TMB oxidation experiments. Reproduced from Paper I.

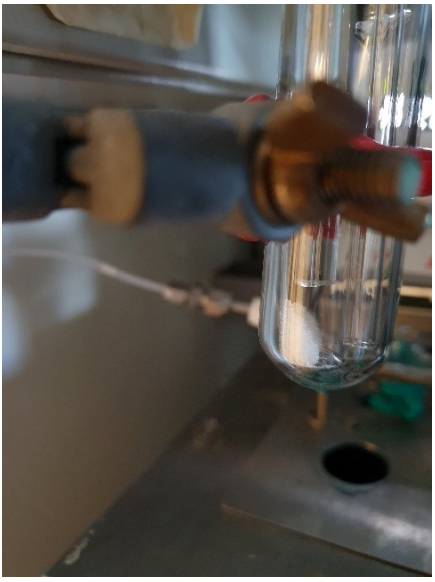

Figure 3.2: N_2O_5 crystals in a diffusion vial fitted with a capillary tube. (Photo: Christian Mark Salvador. Used with permission.)

of a 100cm long and 9.6cm wide quartz glass cylinder which is irradiated over a length of 84 cm by two UV lamps (254 nm). The glass cylinder and the UV lamps are enclosed in a compartment of aluminum mirrors to reduce the inhomogeneity of the photon field. A fan is located at the bottom of the reactor to homogenize air's temperature surrounding the cylinder as well as to keep the temperature low due to potential heat generation by the UV lamps. The VOC is introduced at the center of the flow tube while the oxidants and humidified air are added through a perforated disk distributing them evenly over the cylinder's cross section. The main outflow for analysis is collected via a funnel from the central part of the laminar flow to minimize wall interactions, while the rest of the flow passes through the exhaust line at the bottom of the cylinder (figure 3.1). The median residence time can be adjusted by the total flow.

Ozone and water vapors are introduced into the system to produce OH radicals via the following reactions:

$$O_3 + \mathrm{hv}(\lambda{=}254\mathrm{nm}) \longrightarrow O(^1D) + O_2 \qquad (C\,3.1)$$

$$O(^1D) + H_2O \longrightarrow 2\,OH \qquad (C\,3.2)$$

Ozone is generated by irradiating O_2 with a mercury lamp (λ = 185 nm) outside the PAM reactor.

$$O_2 + \mathrm{hv}(\lambda{=}185\mathrm{nm} \longrightarrow O(^3P) + O(^3P) \qquad (C\,3.3)$$

$$O_2 + O(^3P) \xrightarrow{M} O_3 \qquad (C\,3.4)$$

OH exposure determines how fast the precursor VOCs and their products are oxidized and is expressed as:

$$OH_{exposure} = OH_{concentration} * residence\ time \qquad (3.1)$$

OH concentration can be estimated by using and monitoring the decay of SO_2 under the same RH and initial ozone concentrations as used in experiments (Kang et al., 2007). In this thesis, Go:PAM was also utilized in NO_3-initiated experiments, in which the NO_3 radicals were introduced by dissociation of N_2O_5 via a characterized diffusion source. N_2O_5 synthesized by reacting excess amount of O_3 with pure NO_2 in a mixing glass tube and passing the flow through a cold trap (-78.5 ^{o}C) using dry ice (Faxon et al., 2018). Then the solid N_2O_5 was transferred to a diffusion

vial fitted with a capillary tube inside a glove box. The glove box was filled with N_2 to reduce the relative humidity as much as possible and minimize potential transformation of N_2O_5 to nitric acid (Hallquist et al., 2000). Finally, the N_2O_5 diffusion source was kept in a water bath at a stable temperature, which varied to control NO_3 concentration. The N_2O_5 diffusion source was characterized via NO titration. VOCs were introduced via diffusion vials fitted with capillary tubes and held in a temperature controlled water bath. VOC diffusion fluxes were determined gravimetrically. Go:PAM was used in Paper I, V and the partitioning experiments of NO_3-initiated oxidation of isoprene using neutral and acidic seed aerosol.

3.2 SAPHIR Chamber

SAPHIR (Simulation of Atmospheric Photochemistry In a large Reactor chamber) is a large outdoor chamber (Figure 3.3) in Forchungszentrum Jülich, Germany, which enables studies of atmospheric oxidation of VOCs and the build-up of secondary particles and pollutants.

(a) SAPHIR **(b)** Inside SAPHIR

Figure 3.3: The atmospheric simulation chamber SAPHIR with open roof. I-CIMS was located in the container to the right. (Photo: E. Tsiligiannis).

SAPHIR is a 270 m^3 cylindrical shaped (5 m diameter, 18 m length) double walled TEFLON (FEP) chamber. It is equipped with a shutter system allowing experiments in the dark or in the presence of natural sunlight. The pressure inside the

chamber is kept 45 Pa higher than ambient pressure to prevent any leaks from outside. The space between the two Teflon films is also continuously purged with nitrogen to prevent any contamination from ambient air. In addition, synthetic air is continuously flowing to maintain the over pressure and compensate for the air sampling by the instruments, leading to a small dilution over time. Two fans inside the chamber ensure that the air is well mixed. The low surface area to volume ratio minimizes the wall interactions making SAPHIR suitable for long time scale studies using low – atmospheric relevant – concentrations of trace gases. More details about SAPHIR can be found elsewhere (Rohrer et al., 2005; Fuchs et al., 2012; Fuchs et al., 2017).

SAPHIR was used to simulate nighttime or nighttime-to-daytime transition conditions during the study included in this thesis. The NO_3 radicals were produced in the chamber by the addition of O_3 and NO_2 in the beginning of the experiments, followed by the VOC injection. During a typical experiment more additions of oxidant precursors and injections of VOC were taken place to promote further oxidation (Brownwood et al., 2021; Wu et al., 2021). SAPHIR was used in Paper III, IV and V.

3.3 Chemical Ionization Mass Spectrometry

Mass spectrometry is an online method that can detect individual gaseous ionized molecules in a mixture by separating them according to their mass-to-charge (m/z) ratio. The basic parts of a mass spectrometer consist of an analyte, an ionization source, a mass analyzer, and a detector. There are several techniques to ionize the target molecules; the most common ones used in atmospheric science are electron impact (EI), chemical ionization (CI) and electrospray ionization (ESI) (Laskin et al., 2018).The mass analyzer is used to separate different ionized molecules where quadrupole mass analyzer, time-of-flight (ToF) and ion-trap methods are commonly used in detection and observation of atmospheric molecules. These methods differ in their mass resolving power, which is the ability to distinguish ions of slightly different m/z ratios within a nominal m/z. Finally, the ions are detected in proportion to their abundance by micro-channel plates (MCP) or electron multipliers.

A limitation of mass spectrometry is that it does not provide any structural in-

Table 3.1: Selectivity of different chemical ionization reagent ions used in atmospheric measurements.

Reagent ion	Compounds detected	Reference
I^-	OVOCs, ONs, Halogens and HOMs	(Riedel et al., 2012; Lee et al., 2014)
NO_3^-	H_2SO_4 and HOMs	(Jokinen et al., 2012; Ehn et al., 2014)
Br^-	HO_2 and ONs	(Rissanen et al., 2019; Wu et al., 2021)
CF_3O^-	Peroxides, peroxy acids, and hydroxynitrates	(Crounse et al., 2006; Beaver et al., 2012)
CH_3COO^-	OVOCs and acids	(Veres et al., 2008; Brophy and Farmer, 2016)
H_3O^+	VOCs	(Yuan et al., 2016; Krechmer et al., 2018)
NO^+	VOCs	(Koss et al., 2016)
NH_4^+	OVOCs and HOMs	(Zaytsev et al., 2019)
$(C_2H_5OH)H^+$	amines and amides	(Yao et al., 2016)
$C_6H_6^+$	DMS, isoprene, and terpenes	(Kim et al., 2016; Lavi et al., 2018)

formation about the targeted molecules if it is used alone. Techniques like hydrogen/deuterium exchange (Kostyukevich et al., 2018) or combination of other analytical techniques with mass spectrometry (Claflin et al., 2021; Bi et al., 2021) can be used to obtain information about the chemical structure.

Chemical ionization (CI) is a soft ionization technique, enabling the determination of molecular compositional information by minimizing fragmentation and retaining the original structure of the analyte. CI provides fast time response (~1 Hz) measurements with limits of detection (LOD) of the order of tens of pptv (parts per trillion per volume) and lower, making it a suitable technique for atmospheric applications (Huey, 2007). The ion – neutral molecule (analyte) clustering is the

basic principle for chemical ionization mass spectrometry.

Selectivity and sensitivity of different reagent ions is a key to detecting atmospherically relevant specific compounds or classes of compounds, i.e., with same or similar functionality, without interference from other species (Aljawhary et al., 2013; Riva et al., 2019). Both negative and positive ionization techniques are used in atmospheric science to cover the detection of different compounds. A few examples are presented in Table 3.1. A combination of different CI schemes can be used to describe comprehensively the oxidation evolution of a VOC (Isaacman-VanWertz et al., 2017; Isaacman-VanWertz et al., 2018).

To ionize the reagent ion a radiation source is necessary such as radioactive α particle source (e.g.^{210}Po and ^{241}Am), X-ray source or vacuum ultraviolet light (Ji et al., 2020). Nitrogen is commonly used as carrier gas of reagent ions through the radiation source, where the following reaction take place leading to ionization

$$N_2 \xrightarrow{He^{2+}} {N_2}^+ + e^- \quad \text{(C 3.5)}$$

In this thesis, ${NO_3}^-$ and I^- have been used as the reagent ions during the different studies. ${NO_3}^-$ was used for the 1,3,5-trimethylbenzene (TMB) oxidation experiments focusing on HOM formation, while I^- was utilized for the isoprene oxidation experiments and the ambient observations. However, Paper III describes the product distribution of NO_3-initiated isoprene oxidation using Br^- as the reagent ion. The operation of that instrument as well as the analysis has been done by the Jülich team. The relationship between the Br^- and I^- product distributions will be discussed in section 4.2.

3.3.1 Nitrate (${NO_3}^-$)

Nitrate (${NO_3}^-$) forms clusters with sulphuric acid (Eisele and Tanner, 1993; Kürten et al., 2012) and highly oxygenated organic molecules (HOMs) (Mentel et al., 2015). HNO_3 is ionized by a ^{241}Am α particle source to generate the NO_3 according to the following reaction:

$$(HNO_3)_n + e^- \longrightarrow (HNO_3)_{n-1} \cdot {NO_3}^- \quad \text{(C 3.6)}$$

To minimize sample wall losses, an Eisele type inlet is used to deliver the sample flow to the instrument (Eisele and Tanner, 1993). The sample flow enters the middle part of the inlet while a co-axial laminar sheath flow consisting of particle-free air and the formed NO_3^- ions helps minimize wall losses and ionize the analyte. In addition, a negative voltage applied to the inlet walls prevent wall losses of the ionized analyte molecules. HOMs are detected via adduct formation with NO_3^- (reaction C 3.7) while strong acids like H_2SO_4 can undergo proton transfer reaction as shown in reaction C 3.8.

$$(HNO_3)_{n-1}\cdot NO_3^- + MH \longrightarrow (HNO_3)_{n-1} + NO_3^-\cdot MH \qquad (C\,3.7)$$

$$(HNO_3)_{n-1}\cdot NO_3^- + MH \longrightarrow (HNO_3)_{n-1} + HNO_3^- + M^- \qquad (C\,3.8)$$

3.3.2 Iodide (I^-)

The iodide ions (I^-) are formed by passing methyl iodide (CH_3I) through a ^{210}Po α emitter source (reaction C 3.9) and are suitable for the detection of a variety of species such as inorganic compounds like N_2O_5 (Le Breton et al., 2014b), HNO_3 (Le Breton et al., 2014a) and $ClNO_2$ (Bannan et al., 2015), multifunctional oxygenated or nitrogen-containing compounds (Aljawhary et al., 2013) and HOMs (Lee et al., 2016).

$$CH_3I + e^- \longrightarrow I^- + CH_3 \qquad (C\,3.9)$$

The targeted molecules are mainly detected as adducts with I^- (reaction C 3.10), as I^- is a weak gas phase base and thus proton abstraction and electron donation are insignificant (Lee et al., 2014). The sensitivity of the instrument towards the different iodide-molecule clusters is proportional to the binding enthalpy of the clusters (Iyer et al., 2016). The presence of water in the ion molecule reaction (IMR) chamber (figure 3.4) can affect the sensitivity of the instrument by facilitating or suppressing adduct formation with IH_2O^- clusters. The presence of clustered water is considered to stabilize adduct formation by providing more vibrational modes preventing dissociation (Iyer et al., 2016; Lee et al., 2014).

$$I^-\cdot(H_2O)_n + M \longrightarrow n(H_2O) + MI^- \qquad (C\,3.10)$$

3.3.3 ToF-CIMS

The mass spectrometer used in this thesis has been developed by Aerodyne Research Inc. and Tofwerk and utilizes a time-of-flight (ToF) mass analyzer with the ability

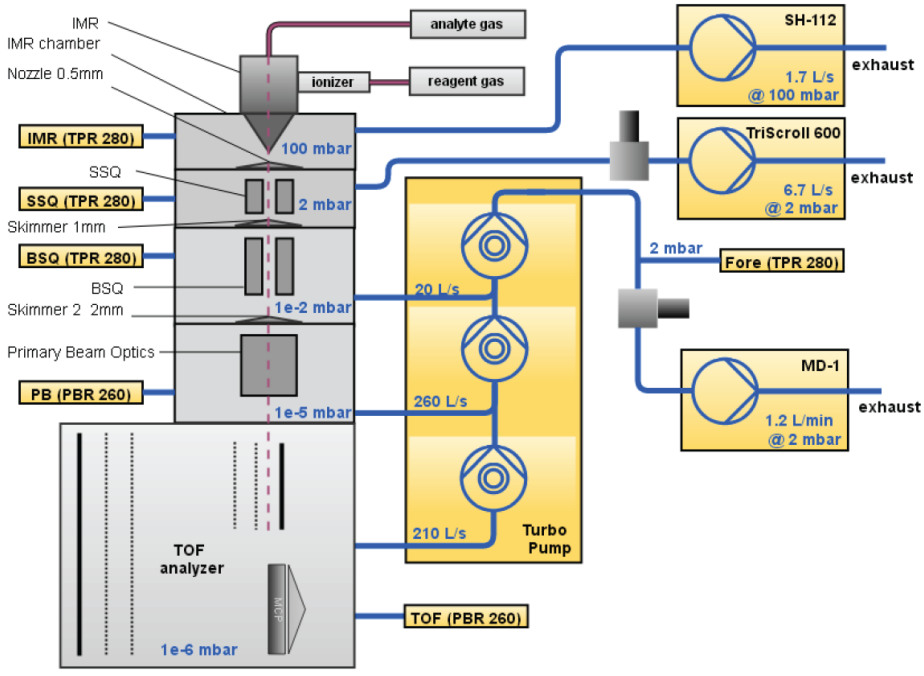

Figure 3.4: Schematic of the ToF-CIMS. Copyright © 2013, TOFWERK AG.

of combining it with different chemical ionization (CI) schemes depending on differences on the front-end of the instrument. The mass spectrometer can be run as an atmospheric pressure interface (API) for detection of charged atmospheric ions (Junninen et al., 2010) or coupled with an Eisele type inlet enabling NO_3^- ionization for measurement of HOMs (Ehn et al., 2014). Alternatively, a low pressure ion molecule reaction (IMR) chamber can be attached at the front-end where the reagent ion and the analyte enter orthogonally to each other, mix in a turbulent flow resulting to adduct formation (figure 3.4). I^- ionization utilizes the IMR chamber (Bertram et al., 2011).

In all cases, the charged ions pumped differentially through the instrument to the ToF mass analyzer. The charged ions go through the short segmented quadrupole (SSQ), the big segmented quadrupole (BSQ) and the primary beam (PB) optic region. In the SSQ region the weakly bound molecular clusters can be dissociate or preserve based on the strength of the electrical field. At BSQ and PB regions the applied voltages and the ion lenses collimate the transmitted ion beam and homogenize the ions energetically, minimizing losses, enhancing transmission, and ultimately increasing sensitivity and resolution. Then, the focused ion beam enters orthogonally the ToF where a direct current pulse of opposite charge accelerates the ions into the ToF pathway. The configuration of the ToF can be adjusted to monitor either positive or negative ions. ToF is also equipped with a reflectron to increase the resolving power up to 5000 (M/ΔM) (Yatavelli et al., 2012).

3.3.4 Calibration

CIMS detects a broad range of compounds depending on the applied reagent ion and the measured signal corresponds to their abundance. However, CIMS provides only information about chemical formulas which can include different isomers. In addition, the technique can have different sensitivity to different isomers, making the quantification of the measured compounds one of the greatest challenges using CIMS.

NO_3^- ionization can detect HOMs and sulphuric acid and the latter is usually used as a calibrant (Ehn et al., 2014). Due to the lack of calibration standards for HOMs the concentration estimations are based on assuming molar yields of HOMs (Jokinen et al., 2014).

I^- ionization is more sensitive to a wider range of molecules compared to NO_3^- ionization making their calibration even more challenging. For organic species with available standards such as simple acids the gravimetric technique can be utilized to determine a sensitivity factor. Also, inorganic species like N_2O_5 and $ClNO_2$ can be directly calibrated via NO titration. However, these processes are time consuming and usually difficult to perform during ambient measurements. Nevertheless, the largest obstacle is the lack of standards for most of the measured molecules.

A new technique called voltage scanning (VS) has been used to simplify this process by estimating an upper limit sensitivity. This gives a lower limit of concentration of the corresponding species, based on the collision limit of iodide ion adducts (Lopez-Hilfiker et al., 2016; Iyer et al., 2016). However, the detected species during this approach fall along the declustering curve adding uncertainty in the estimated calibration factors.(Bi et al., 2021) have found that the estimating sensitivity of a given compound using VS can vary 0.5 to 1 order of magnitude. But the VS technique can be used to estimate a sensitivity of summed compounds with low error around 30 %.

3.4 FIGAERO inlet

ToF-CIMS measures only compounds in the gas phase. Different inlets can be coupled to the instrument to retrieve molecular information about the compounds in the particle phase (Lopez-Hilfiker et al., 2014; Lopez-Hilfiker et al., 2019). The Filter Inlet for Gases and AEROsols (FIGAERO) is an inlet which allows for simultaneous semi-continuous measurements of compounds in gas and particle phase (Lopez-Hilfiker et al., 2014; Thornton et al., 2020).

The FIGAERO operates in two main modes: gas phase measurement with simultaneous particle collection on a 25mm 1µm PTFE filter and thermal desorption of the collected particles and determination of particle molecular composition (figure 3.5). It consists of two sampling ports and a thermal desorption port to avoid any cross-contamination. An automated movable tray switches between the sampling/collection mode and the desorption one. The duration of stage can be adjusted automatically depending on the sampling conditions. During desorption ultrahigh pure nitrogen passes through the heating tube increasing gradually the temperature right above the filter while the resulting vapors are sampled and analyzed by the CIMS. The desorption temperature is typically ramped from room temperature up to 200 ^{o}C, followed by a soak period at 200 ^{o}C to ensure all material has evaporated and allow the signals to return to initial levels. The desorption profile, also called thermogram, provides information about the volatility of a specific compound by relating the maximum temperature (T_{max}) of the desorbed signal to the vapor pressure (Thornton et al., 2020).

3.4.1 Particle phase calibration

FIGAERO can be used to extract vapor pressures of the components of desorbed particles via thermograms. The volatility calibration can be done using solutions of known concentration of the measured compounds. Solutions of carboxylic acids and polyethylene glycol (PEG) of different sizes are widely used to determine a calibration curve covering a range of vapor pressures (Bannan et al., 2019). The calibration is commonly done by the syringe deposition method in which the FIGAERO filter is doped with freshly prepared solution standards followed by the desired thermal desorption profile. However, discrepancies between different studies using the aforementioned method led to a suggestion of a new method for volatility calibration by using atomized calibration compounds (Ylisirniö et al., 2021). Nevertheless, uncertainties still remain, especially, when it is used for the determination of volatility of HOMs and oligomers, as they may be subject to thermal decomposition (Schobesberger et al., 2018).

3.5 CIMS data analysis

The ToF-CIMS data were processed using the Tofware software package (www.tofwerk.com/tofware) written in Igor Pro software (Wavemetrics Inc.,OR, USA) (Stark et al., 2015). The raw data are recorded every second while a pre-averaging process to 10 sec, 1 min, 10 min or 1h depending on the application was taken place before analysis to optimize processing time and increase the signal-to-noise ratio.

The initial step of data processing is the mass calibration. Mass calibration is critical as accurate mass calibration enables correct peak assignments. Generally, this includes known peaks such as the reagent ion peaks (I^- , IH_2O^- and I_3^-), common dominant acids like nitric, formic, acetic and lactic acids, mass calibrants like perfluorinated pentanoic or heptanoic acid (PFPA or PFHA) as well as experimental contaminants associated with sampling lines. A key on choosing the right mass calibrants is to avoid calibrants that create double peaks, as this will influence the determination of the calibrated peak shape, and consequently the peak fitting.

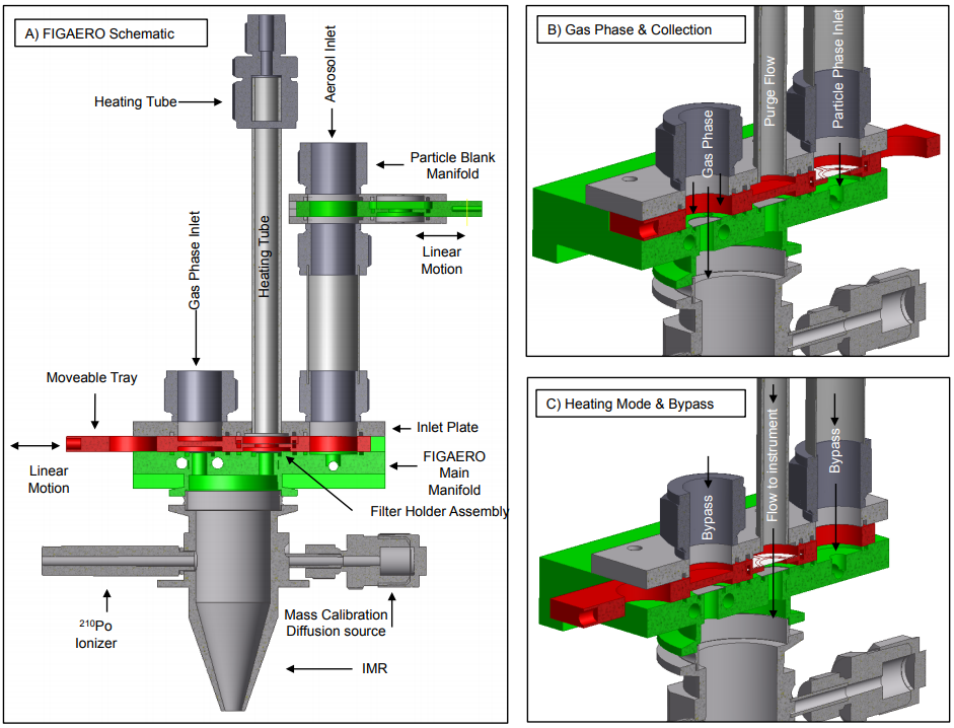

Figure 3.5: FIGAERO schematics. A) FIGAERO overview. The main manifold (green) and the movable tray (red) are made of Teflon. The movable tray switches between the two modes. The two sampling ports (gas phase inlet and aerosol inlet) and the thermal desorption port connected to the eating tube are mounted at the inlet plate. B) FIGAERO during gas phase sampling and particle collection. The desorption port is blocked by the tray. C) FIGAERO during desorption. The filter holder moves under the heated N_2 stream while the gas sampling port is blocked by the tray. Reproduced from (Lopez-Hilfiker et al., 2014).

3.6 Other instruments

A few auxiliary instruments were utilized during the experiments. Briefly, the following instruments were used: a scanning mobility particle sizer (SMPS, 3080 TSI) to measure particle number distributions, a condensation particle counter (CPC,

3775 TSI) to monitor the number of particles, an ozone monitor (2B Technologies, model 205), a NO_xbox (Thermo Scientific, model 42i monitor), a SO_2 monitor (Teledyne T100) and relative humidity and temperature probes (Vaishala HMP60).

4

Results and Discussion

Contents

Chapter 4 answers the research questions presented in section 1.3 and summarizes the results of five peer-reviewed papers (Papers I – V) and discusses the results of partitioning experiments of NO_3-initiated isoprene oxidation using neutral and acidic seed aerosol. It consists of three sections. The first focuses on nitrogen-containing oxidation products from anthropogenic VOC (TMB) (Paper I) and activities (nitro-aromatic compounds) (Paper II), the second section discusses the organonitrates (ON) formed by oxidation of biogenic VOC (isoprene) (Paper III – V), and the last one deals with the role of the aforementioned nitrogen-containing oxidation products on SOA formation (Paper I & partitioning experiments).

4.1 Nitrogen-containing compounds from aromatics

The main focus of this section is on a laboratory study of OH oxidation of TMB under different NO_x conditions (Paper I). Furthermore, ambient observation of nitro-aromatics arising from human activities in a rural area will be discussed (Paper II).

4.1.1 ON formation from TMB under different NO_x conditions

Highly oxygenated organic molecules (HOM) have been observed in OH oxidation of aromatic systems under NO_x-free conditions (Wang et al., 2017; Molteni et al., 2018) prior to Paper I, while after Paper I a few studies were published on HOM formation from different aromatics with and without NO_x addition (Garmash et al., 2020; Wang et al., 2020; Mehra et al., 2021; Priestley et al., 2021; Cheng et al., 2021).

The OH oxidation experiments of TMB described in Paper I were conducted using the Gothenburg potential aerosol mass (Go:PAM) laminar flow reactor (Watne et al., 2018). The experiments were done using a constant TMB initial concentration under different amounts of OH radicals and elevated NO_x concentrations (table 4.1). The experiments were divided into the NO_x-free experiments (A small concentration

of NO_x was monitored, 3-5 ppb, probably stemming from NO contamination) and the NO_x experiments. NO_x concentrations were adjusted at $[NO_x]_0 : [VOC]_0$ ratios representative to polluted urban areas (Ran et al., 2009). TMB oxidation was simulated using a kinetic box model based on MCM v3.3.1 (Jenkin et al., 1997) and an additional general scheme for HOM formation (Ehn et al., 2014; Wang et al., 2017; Kroll et al., 2011; Berndt et al., 2018; Zhao et al., 2018) to predict the lumped product distribution.

The oxidation products can be classified into monomers, containing the nine carbons from the original TMB, and dimers containing eighteen carbon atoms under NO_x-free conditions. Minor fragmentation, i.e. compounds with less than nine or eighteen carbons, was observed. The classified HOM monomers had the general formula of $C_9H_{12\text{-}16}O_{6\text{-}11}$, while the HOM dimers had chemical formulas of $C_{18}H_{24\text{-}30}O_{10\text{-}16}$. Following the proposed termination scheme by (Mentel et al., 2015), compounds can be classified into families (table 4.2). Monomers with even number of hydrogens are closed shell products whilst monomers with odd number of hydrogens are radicals. Monomers with 12 H atoms can be classified as first-generation products terminated by $C_9H_{13}O_x$ radicals while compounds with 16 H atoms as second-generation products terminated by $C_9H_{15}O_x$ radicals. Monomers with 14 H atoms can be either first or second-generation products originating from both $C_9H_{13}O_x$ and $C_9H_{15}O_x$ radicals. First-generation products ($C_9H_{12}O_x$) had the highest contribution at low OH exposure, while $C_9H_{14}O_x$ and the second-generation products ($C_9H_{16}O_x$) increased with increasing OH exposure reaching their highest contribution at experiment 4. HOM Dimers can be formed via the general reaction:

$$HOMRO_2 + HOMRO_2 \longrightarrow HOMDIMER + O_2 \qquad (C\,4.1)$$

Similarly, dimers with 26 H atoms were classified as first-generation products, the ones with 30 H atoms were second-generation ones and the compounds with 28 H atoms can be either first or second-generation dimers.

The rate of dimer formation depends on the square of [HOM-RO_2] and their contribution will increase with high RO_2 concentrations. HOM-RO_2 distribution is important on formation of dimers, especially in flow tube reactors. High OH levels lead to rapid consumption of TMB resulting to high RO_2 concentrations, and subsequently HOM-RO_2 formation and their relative importance can drive dimer formation (figure 4.1). Dimer contributions were highest at high OH exposure (experiments 3 and 4). Dimers with 28 H atoms had the highest contribution at

Table 4.1: Experimental conditions for experiments with 30 ppb TMB. Ozone and initial NO_x concentration at time zero are given in parts per billion (ppb) and explicitly modelled OH exposure in number of molecules second per cubic centimeter (molec s cm^{-3}). TMB reacted (ΔTMB) in parts per billion (ppb) after a reaction time of 34 s and particle number concentration given in no. cm^{-3} after reaching steady state in the Go:PAM. RH in all experiments was 38 %. Reproduced from Paper I.

Exp.	$[O_3]_0$	$[NO_3]_0$	**OH exposure**	**ΔTMB**	**NO_x/ΔTMB**	**Particle number**	**Contr. top - 10 species (%)**
1	~19	5	$3.5x10^9$	5.4	0.9	-	28.6
2	~19	5	$7.1x10^9$	9.9	0.5	-	29.8
3	~100	3	$3.8x10^{10}$	26	0.1	60±14	38.6
4	~100	3	$2.1x10^{11}$	30	0.1	1610± 217	35.9
NO_x9	~9	82	$6.3x10^9$	9	9.1	-	52.4
NO_x3_L	~12	38	$7.9x10^9$	11	3.5	-	42.3
NO_x3_H	~100	79	$3.1x10^9$	25	3.2	-	34.2
NO_x1	~100	35	$9.1x10^{10}$	30	1.2	170±50	30.5

all NO_x-free experiments, apart from the experiment with the lowest OH exposure (experiment 1) in which the first-generation products ($C_{18}H_{26}O_x$) were the dominant ones. The second-generation dimers ($C_{18}H_{30}O_x$) contribution was generally quite lower, and they had the highest fraction in experiment 4. The contribution of monomers to the total product signal ranged from 33.1%-42.1% and the dimers from 25.4% to 43.3% at the NO_x-free experiments.

In addition to HOM monomers and dimers, nitrogen-containing C_9 compounds with one or two N atoms and C_{18} compounds with only one N atom were identified during the experiments with elevated NO_x (figure 4.1). These products are expected to be organonitrates (ONs) or peroxy nitrates, as it is highly unlikely to form nitro-aromatic compounds from TMB (Sato et al., 2012). The nitrogen-containing products had the general formulas $C_9H_{12\text{-}18}NO_{6\text{-}13}$, $C_9H_{12\text{-}18}N_2O_{8\text{-}15}$ and $C_{18}H_{18\text{-}24}NO_{6\text{-}10}$. The dominant ONs were $C_9H_{13}NO_8$, $C_9H_{15}NO_{10}$ and $C_9H_{14}N_2O_{10}$. Nitrogen-containing compounds dominated the spectra and had

Table 4.2: Contribution of oxidation products families to the total signal. Reproduced from Paper I.

Compound family	**1**	**2**	**3**	**4**	**NO_x9**	**NO_x3_L**	**NO_x3_H**	**NO_x1**
$C_9H_{12}O_x$	11.3	7.8	3.5	5.4	8.5	9.3	5.9	5.4
$C_9H_{13}O_x$	5.7	4.5	3.3	2.1	6.0	7.0	5.6	4.2
$C_9H_{14}O_x$	8.3	10.8	9.9	17.4	4.3	6.6	8.0	13.0
$C_9H_{15}O_x$	5.6	7.2	9.4	4.1	2.4	3.3	4.6	4.7
$C_9H_{16}O_x$	4.8	8.0	7.7	14.5	1.5	2.5	4.8	10.3
$C_{18}H_{26}O_x$	8.5	9.1	8.5	9.3	0.8	2.0	2.7	6.0
$C_{18}H_{28}O_x$	7.1	9.9	9.3	11.0	0.4	1.2	2.6	6.9
$C_{18}H_{30}O_x$	0.7	1.0	2.3	2.6	0.4	0.4	0.9	1.7
$C_9H_{13}NO_x$	6.2	4.7	0.6	0.6	26.8	17.1	10.1	4.8
$C_9H_{15}NO_x$	6.4	5.6	0.7	0.9	3.7	10.3	14.5	8.5
$C_9H_{14}N_2O_x$	2.1	1.7	1.0	1.1	18.7	11.8	7.5	1.9

the highest contribution compared to monomers and dimers in all NO_x experiments, apart from the experiment NO_x1 with the smallest amount of NO_x added and a high OH exposure. The amount of nitrogen-containing compounds increased with elevated NO_x at the expense of HOM monomers and especially HOM dimers. The ONs contribution ranged from 38.4% to 72.5%. The fractions of monomers and dimers to the total product signal reduced to 20.7% and 6.8%, respectively, in experiment NO_x9 which had the highest NO_x initial concentration and one of the lowest OH exposures. The changes in the product distribution can be explained as the reaction of RO_2 + NO resulting to ONs competes efficiently the termination pathways of autoxidation, RO_2 + RO_2 and RO_2 + HO_2. The observed first-generation ONs ($C_9H_{13}NO_x$) can be formed via the following reaction pathway:

$$C_9H_{13}O_{5-11} + NO \longrightarrow C_9H_{13}NO_{6-12} \qquad (C\,4.2)$$

On the other hand, the second-generation nitrogen-containing compounds ($C_9H_{15}NO_x$) can be formed from different pathways. The termination of a second-

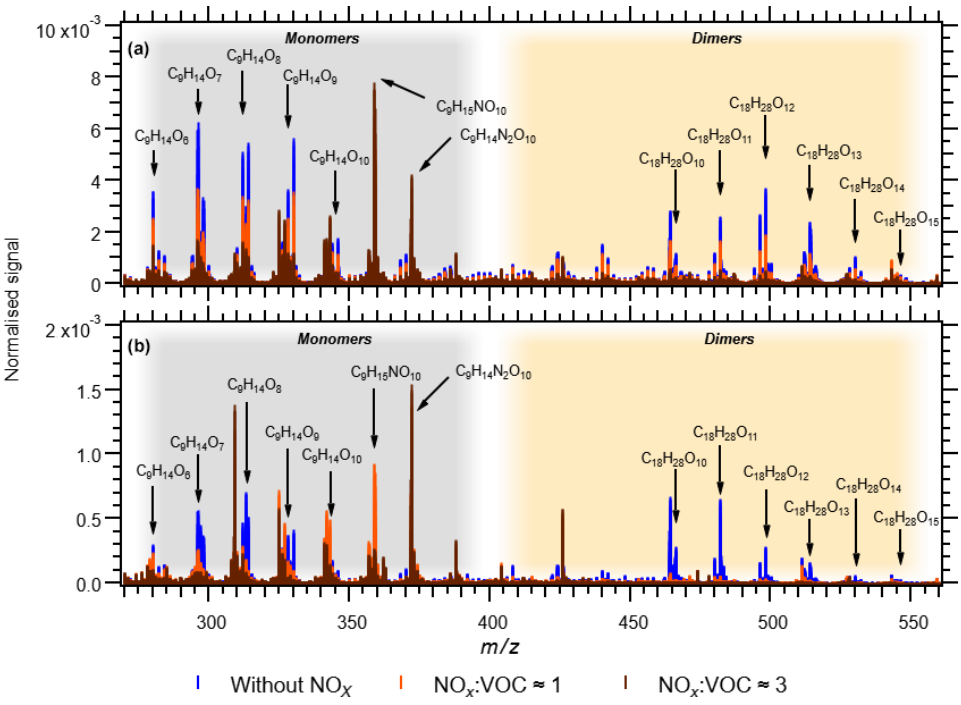

Figure 4.1: Comparison of mass spectra of HOM and nitrates. Panel (A) shows experiments 4 (blue), NO_x1 (orange) and NO_x3_H (brown). Panel (B) shows experiments 2 (blue), NO_x3_L (orange) and NO_x9 (brown). Reproduced from Paper I.

generation peroxy radical ($C_9H_{15}O_x$) by NO leads to $C_9H_{15}NO_x$ (reaction C 4.3). In addition, the reaction of a first-generation nitrate by OH radicals, followed by an autoxidation step and termination either by peroxy (reaction C 4.4) or by hydroperoxy radicals (reaction C 4.5) can result to $C_9H_{15}NO_x$ formation.

$$C_9H_{15}O_{7-11} + NO \longrightarrow C_9H_{15}NO_{8-12} \quad \text{(C 4.3)}$$

$$C_9H_{14}O_{9-13} + RO_2 \longrightarrow C_9H_{15}NO_{8-12} + R = O + O_2 \quad \text{(C 4.4)}$$

$$C_9H_{14}O_{8-12} + HO_2 \longrightarrow C_9H_{13}NO_{8-12} \quad \text{(C 4.5)}$$

OH attack on a first-generation nitrate ($C_9H_{13}NO_x$) and subsequent termination of the formed RO_2 by NO (reaction C 4.6) is necessary for the formation of the most

abundant dinitrates ($C_9H_{14}N_2O_x$).

$$C_9H_{14}O_{7-11} + NO \longrightarrow C_9H_{14}N_2O_{8-12} \quad (C\,4.6)$$

Finally, the reaction of RO_2 with NO_2 and formation of peroxy nitrates (PAN-like compounds) (reaction C 2.29) cannot be ruled out as a potential nitrate formation pathway. The results of the simplified kinetic box model followed the observed behavior of the lumped monomers, dimers, and nitrates under the different experimental conditions. A few rate coefficients were applied on dimer formation and termination of HOM-RO_2 by NO to compare to the experimental results. The use of the rate coefficient on dimer formation proposed by (Zhao et al., 2018) (2.0 x 10^{-12} cm^3 $molec^{-1}$ s^{-1}) and the rate coefficient (1.0 x 10^{-11} cm^3 $molec^{-1}$ s^{-1}) from (Berndt et al., 2018) for HOM-RO_2 + NO showed the better representation between the measured and predicted bulk fractions of monomers, dimers, and nitrates.

4.1.2 Ambient – Nitro-aromatic (China)

A group of compounds that is considered to originate exclusively from anthropogenic sources are nitro-aromatic compounds (NAC). NAC are aromatic compounds with at least one nitro (–NO_2) functional group attached directly to a benzene ring. NAC can be attributed to various primary sources, such as biomass burning and vehicle emissions, as well as secondary oxidation of VOCs containing a benzene ring (Wang et al., 2019; Mehra et al., 2021).

16 NACs were identified both in gas and particle phase during an ambient campaign in rural China (Paper II), and further classified into four sub-groups based on their similarities to nitrophenol (NP), nitrocatechol (NC), nitrobenzoinc acid (NB) and dinitrophenol (DNP). Overall the sub group NP contributed almost 50%, followed by NC and with smaller fractions of DNP and NB. Intensive biomass burning (BB) episodes were observed during the campaign and were used to divide the measurements into BB and non-BB regimes in order to assign sources to the lumped sub-groups. The three representative NACs (NP, NC and DNP) behaved quite differently under the regimes linked to strong BB events (figure 4.2). NP concentrations clearly increased both in the gas and particle phase during the BB events, indicating that NP and its analogues were good direct tracers of primary

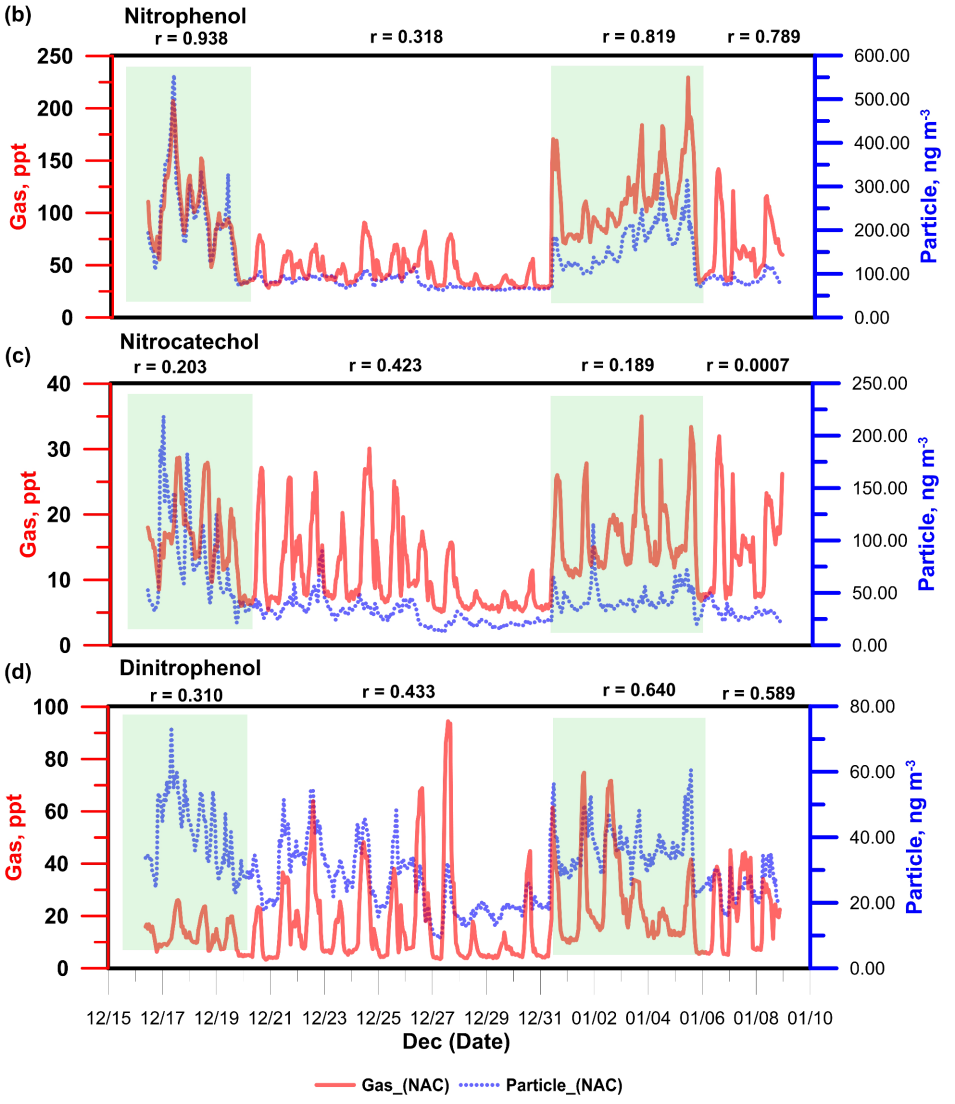

Figure 4.2: Mixing ratios of (b) nitrophenol, (c) nitrocatechol, and (d) dinitrophenol under regimes corresponding to BB episodes (colored areas) and non-BB episodes. The coefficient of correlation (r) reflects the agreement between the gas- and particle-phase concentrations. Adapted from Paper II.

emissions from BB. NC and DNP time behavior did not show a pattern between BB events and non-BB events and their correlations between the gas and the particle phase were very weak compared to NP correlations.

During non-BB events all NACs correlated with ozone concentrations, suggesting that secondary photochemical processes were the dominant NAC formation pathway. NP correlation with ozone was strong for non-BB regimes but very poor if the full data set was taken in account, supporting the argument that during BB events the primary combustion emissions were the major source of NP. On the other hand, the correlation of determination of NC and DNP with ozone was quite similar for both cases, i.e. non-BB regimes data and full data set. This suggests that the formation pathways of these compounds were mainly via secondary oxidation and did not change largely over time, regardless of the occurrence of BB episodes.

4.2 Organonitrate formation from isoprene

This section focuses on organonitrates (ONs) formed from the oxidation of isoprene by nitrate (NO_3) radicals. Results from the extensive experimental campaign in SAPHIR chamber (Paper III and IV) where the nighttime oxidation of isoprene was simulated will be presented while their connection to ambient observations will be also discussed (Paper V). An I-CIMS and a Br-CIMS were running during the campaign. This thesis work based on the I-CIMS measurements but results using the Br-CIMS will also be discussed as Paper III based on Br-CIMS measurements. I-CIMS was located in an air-conditioned container under the chamber. A four-meter long PFA line and four-meter long copper tubing were used as gas and particle inlets, respectively. Br-CIMS was coupled with a customized inlet (Albrecht et al., 2019) and attached directly at the bottom of the chamber minimizing losses (Paper III). I-CIMS was also operated with FIGAERO inlet during the campaign, but no particle phase results will be discussed.

A broad range of conditions applied during the campaign to test different chemical loss pathways of RO_2. In general, the dominant RO_2 loss in all experiments was the reaction with HO_2.

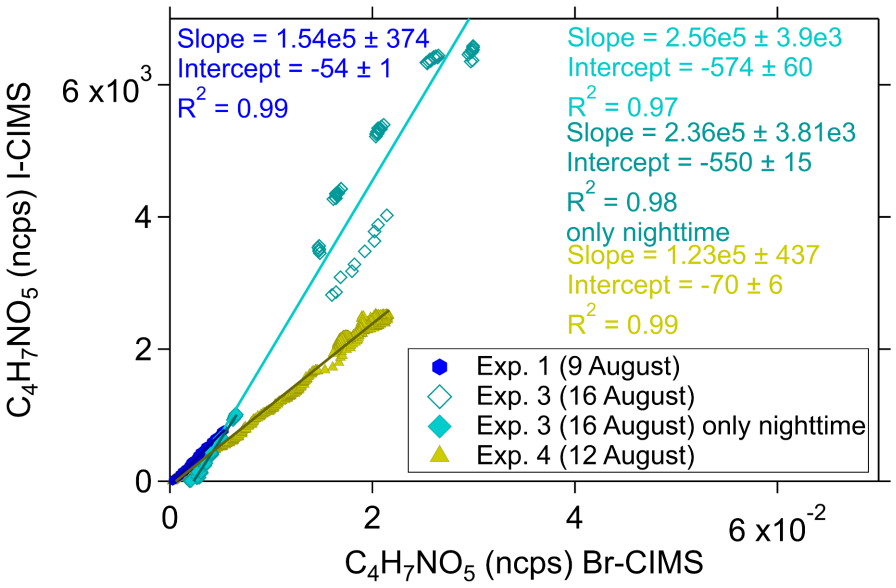

Figure 4.3: Comparison of $C_4H_7NO_5$ measurements by I-CIMS and Br-CIMS. Adapted from Paper V.

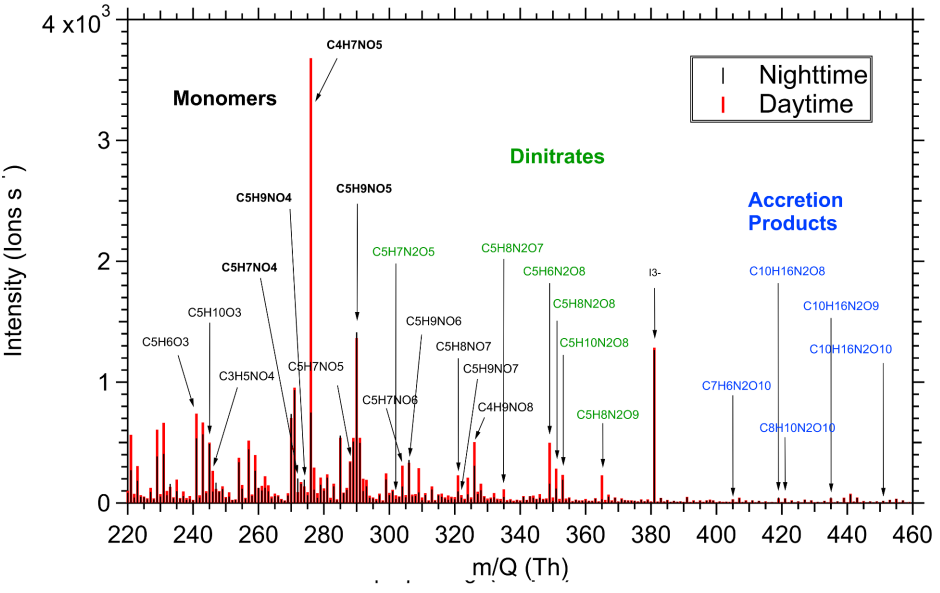

Figure 4.4: Representative I-CIMS data. Experiment 16^{th} of August at humid and low NO_3 conditions with ammonium sulfate aerosol seeds.

However, a relative enhancement of RO_2 + RO_2, RO_2 + HO_2 reactions or RO_2 isomerization was achieved. Nighttime-to-daytime transition has been also studied in some experiments, while unseeded and seeded experiments were also conducted. (see Paper IV for the full list). Sixty-four ONs identified by I-CIMS during the experiments. ONs consisted of monomers (C_5), products after fragmentation, and accretion products with one or two nitrogen atoms. One monomer and three accretion products with three nitrogen atoms were also detected. Some compounds, containing only C, H and O atoms, such as $C_5H_8O_{2,3}$, were also found. Br-CIMS detected more 3-N monomers ($C_5H_9N_3O_{10\text{-}12}$) and dimers ($C_{10}H_{17}N_3O_{12\text{-}16}$) compared to I-CIMS likely due to fewer inlet losses. In general, I-CIMS and Br-CIMS measurements were well linearly correlated, especially during the initial oxidation steps (figure 4.3). However, the correlation coefficients differed from experiment to experiment. This can be due to deviations in the operational characteristics, such as IMR pressure, from day to day as well as formation of different isomers because of the different experimental conditions. It is not known how sensitive the I^- and Br^- ionization schemes to different isomers are. I-CIMS was also operated with FIGAERO inlet during the campaign, but no particle phase results will be discussed.

Mononitrates dominated the I-CIMS spectrum ranging from around 80 – 96% of the measured ONs, assuming equal sensitivity to all identified species (figure 4.4). Dinitrate followed with a relative contribution of 3 – 18% while the fraction of accretion products was less than 2%. The major mononitrates had the chemical formulas $C_5H_{7,9}NO_{4\text{-}7}$, while the 1-N products from fragmentation with a significant contribution were $C_4H_7NO_{5,6}$ and $C_3H_5NO_4$. Dinitrates $C_5H_{6,8,10}N_2O_{8,9}$had the most substantial signal intensities whereas the most abundant accretion products were the dimers with molecular formulas $C_{10}H_{16}N_2O_{8\text{-}10}$.

The time evolution of the products provides insights on the degree of oxidation and on characteristics about their formation pathways. The oxidation state of carbon (Kroll et al., 2011) increased during the experiments. The bulk averaged carbon oxidation state in the experiment discussed in Paper III was -0.35 after the first isoprene injection and increased up to 0.09 in the end of the experiment indicating the formation of more oxidized products after a few hours of oxidation. 1-N monomers consisted mainly of first-generation products, i.e. stemming from different termination pathways of the initial produced peroxy radical from the first attack of NO_3 at the isoprene double bonds. The initial nitrooxy peroxy radical can undergo autoxidation forming more oxidized radicals before getting termi-

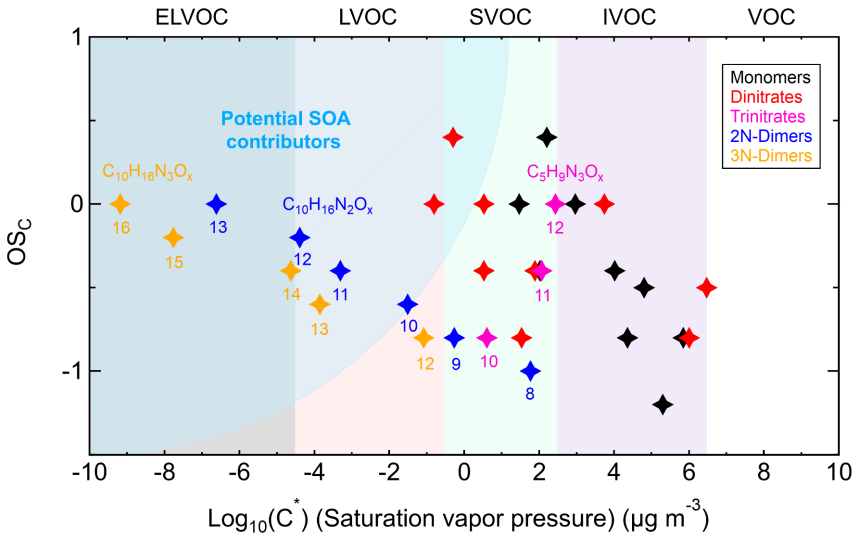

Figure 4.5: Volatility distribution of different organonitrates formed from NO_3-initiated isoprene oxidation. The volatility classes are indicated along the top with corresponding colors in the plot. The position of potential SOA contributors is determined depending on the exact functionalities of molecules adapted from (Bianchi et al., 2019). Reproduced from Paper III.

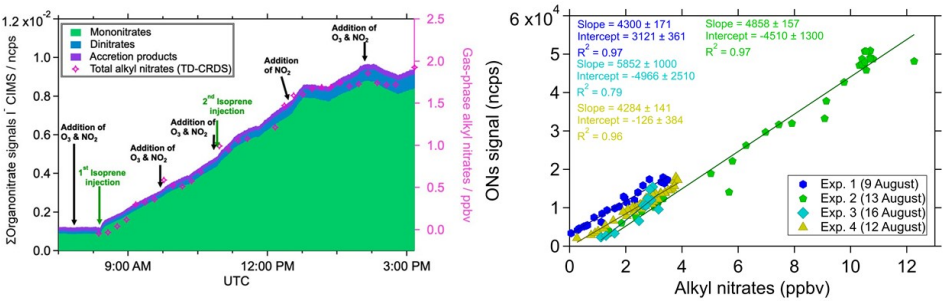

Figure 4.6: (Left) Time series of classes of summed ONs measured by I-CIMS compared to total And time series. Adapted from Paper IV. (Right) Total ONs signal detected by I-CIMS versus alkyl nitrates measured by the TD-CRDS. Adapted from Paper V.

nated, can also react with HO_2 or another peroxy radicals. The reaction between two peroxy radicals can yield dimers containing two nitrogen atoms.The alkoxy radicals produced from the RO_2 + RO_2 and RO_2 + HO_2 reactions can undergo

unimolecular rearrangement by H shift and O_2 addition leading to new RO_2 radicals or they can decompose making fragments. Most of the 1-N monomers increased directly after every isoprene injection indicating that their signals were dominated by first-generation products. Few 1-N monomers, like $C_5H_9NO_7$, governed by second-generation products according to their time evolution measured by CIMS. Similarly to most 1-N monomers, 2-N dimers also formed rapidly in the beginning of isoprene additions and then declined implying that the measured signals comprised mostly first-generation products. Fragmentation products with one nitrogen atom showed a secondary formation behavior by increasing slowly and steadily during the experiments. Dinitrates considered second-generation products as they formed after a second NO_3 attack to the remaining double bond of the primary products. Their time evolution clearly demonstrated this as their relative contribution was increasing gradually and maximized towards the end of the experiments after all isoprene has consumed.

One unseeded and one seeded experiment with similar chemical conditions were used to estimate the saturation vapor pressures of specific products in Paper III in conjunction with composition-activity (Donahue et al., 2011; Mohr et al., 2019; Peräkylä et al., 2020) and group-contribution (Nannoolal et al., 2008; Pankow and Asher, 2008; Compernolle et al., 2011) semiempirical methods. The molecular information about the functional groups and structures needed for the calculations derived by the mechanistic formation pathways for different compounds. The volatility distribution of ONs formed by NO_3-initiated isoprene oxidation showed that 1N-monomers fell in the IVOC or SVOC range. The 2N and 3N-monomers volatilities ranged from IVOC to LVOC with most of them being in the SVOC class. Dimers were less volatile spanning from SVOC to ELVOC classes (figure 4.5).

The total alkyl nitrates (ANs) was measured by a Thermal Dissociation Cavity Ring-Down Spectrometer (TD-CRDS) during the experiments (Paper IV). The alkyl nitrate molar yield based on isoprene consumption by NO_3 estimated to be (108 ± 15) % and largely independent of the initial conditions explored. The time evolution of the bulk AN yield was in good agreement with the summed signal of ONs measured by I-CIMS (figure 4.6 (Left)), suggesting the CIMS total ONs signal included the majority of the formed ON. This enables an estimation of a bulk ON sensitivity assuming the same sensitivity for all the measured ONs. A mean average bulk ON sensitivity of 4.8 ncps ppt^{-1} with a standard deviation of 0.7 ncps ppt^{-1} was estimated for selected experiments ((figure 4.6 (Right)) and used to convert the measured ONs signal to concentrations in Paper V.

4.2.1 Major ONs from isoprene oxidation. Lab vs Ambient

Paper V presents the behavior of the major produced ONs during selected experiments in SAPHIR chamber in conjunction with ambient observations. $C_4H_7NO_5$ was detected by CIMS as an important nitrated tracer together with the primary products $C_5H_9NO_5$ (hydroperoxide nitrates, INP), $C_5H_7NO_4$ (carbonyl nitrates, ICN), and $C_5H_9NO_4$ (hydroxy nitrates, IHN). $C_4H_7NO_5$ can consist of at least four isomers and the signal increased slowly and steadily during the NO_3-dominated nighttime oxidation, suggesting that there was not any major sink. However, the yield of $C_4H_7NO_5$ was strongly dependent on the chemical regime. The dominant loss of RO_2 was the reactions with HO_2 or NO_3 during the experiments, nevertheless relative enhancement of the RO_2 + RO_2 pathway was achieved in different experiment. The relative formation yield of $C_4H_7NO_5$, expressed as the ratio of $C_4H_7NO_5$ over the total measured ONs signals by CIMS enhanced when RO_2 loss favored RO_2 + RO_2 reactions compared to RO_2 + HO_2 reactions. The relative contribution of $C_4H_7NO_5$ to total measured ONs ranged from 5% up to 17% under nighttime oxidation.

Two experiments were used to simulate nighttime-to-daytime transition, after all isoprene has consumed, and follow the fate of the products. The daytime conditions were either favored oxidation by OH or reducing OH concentration by scavenging OH radicals by CO addition favoring only photolysis. Isoprene-derived carbonyl nitrates are expected to decrease under daytime and low NO conditions, as they react with OH radicals or are rapidly photolyzed (Müller et al., 2014; Xiong et al., 2016)). However, the signal of $C_4H_7NO_5$ did not decrease, instead there was a strong increase from 10% at the end of nighttime to over 40% after an hour of OH oxidation making $C_4H_7NO_5$ the most dominant ON. During the experiment with added CO, i.e. mostly photolysis, the $C_4H_7NO_5$ enhancement was smaller, and its relative contribution increase up to 22%. The lack of isoprene during daytime clearly confirms the importance of multi-generational sources of $C_4H_7NO_5$.

$C_4H_7NO_5$ and the other major ONs ($C_5H_9NO_5$, $C_5H_7NO_4$, and $C_5H_9NO_4$) observed in the chamber experiments were characterized in six different field campaigns around the world. Ambient observations took place in Asia; one in Changping (near Beijing), China (Le Breton et al., 2018b) and the other in Hong Kong (Peng et al., 2022). Two sites were located in Europe, in Jülich, Germany, and in Gothenburg, Sweden.

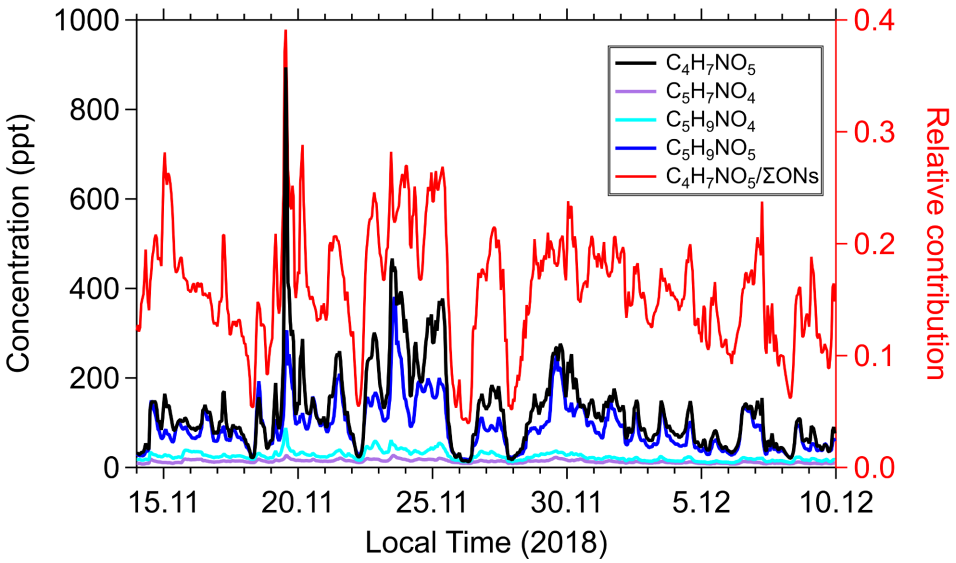

Figure 4.7: The time series of the major isoprene nitrates in Hong Kong. The relative contribution represents the ratio of $C_4H_7NO_5$ over the total isoprene-derived nitrates that measures via the I-CIMS during the campaign. Adapted from Paper V.

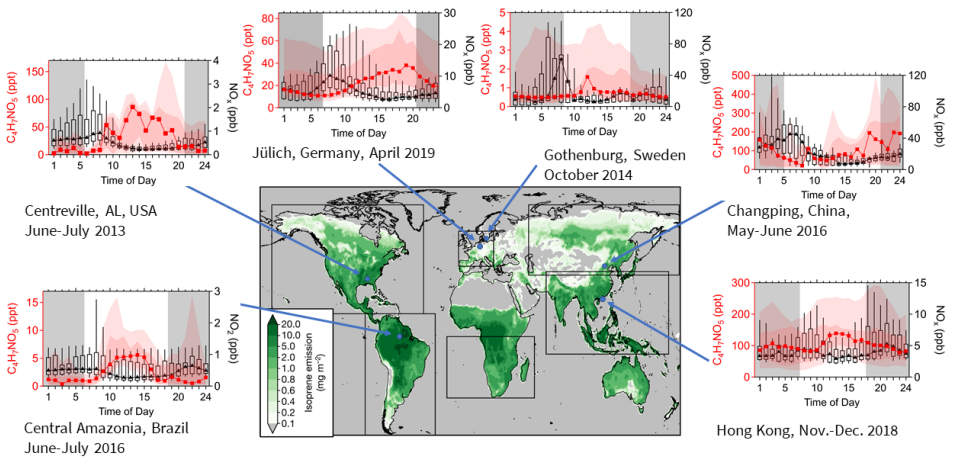

Figure 4.8: Median diurnal profile of the $C_4H_7NO_5$ and NO_x for six different locations, with the 10^{th}, 25^{th}, 75^{th} and 90^{th} percentile. The grey areas in the plot indicate the nighttime period. For Amazonia only the NO_2 was available. The map with the isoprene emissions is adapted from McFiggans et al. (2019). Reproduced from Paper V.

Finally, data from Alabama, in the south-eastern USA (Lee et al., 2016) and from central Amazonia, Brazil were used to illustrate the omnipresence of the $C_4H_7NO_5$ isomers. In contrast to chamber measurements where $C_4H_7NO_5$ compound(s) were significantly produced in the night and further enhanced, and clearly dominated during daytime, the ambient observations of the $C_4H_7NO_5$ signal showed that it was the dominant isoprene-derived nitrate measured both during daytime and nighttime at all the sampling sites (figure 4.7). However, the diurnal profile of $C_4H_7NO_5$ differed at different locations (figure 4.8).

In Hong Kong – an isoprene-rich area with influence from anthropogenic emissions (Peng et al., 2022) – $C_4H_7NO_5$ had two peaks, one during daytime and one during nighttime. The nighttime peak becomes more prevalent if only a period with high isoprene-derived ONs is selected. In Changping (near Beijing), China $C_4H_7NO_5$ profile was different. There was a higher contribution during night than during day in conjunction with higher variability. Overall, isoprene concentrations were almost always above zero, even during nighttime, with a peak of the mean diurnal profile at 14:00 (Le Breton et al., 2018a). Air masses reaching Beijing area are strongly influenced by the local meteorology, e.g., the wind speed has high values during the day and low values during the night (Le Breton et al., 2018b). In Europe, $C_4H_7NO_5$ had a clear wide peak in the early evening in Jülich, Germany, whilst there was a weak peak around noon in Gothenburg, Sweden. In general, these two sites are characterized by low regional isoprene emissions, but they influenced from human sources. Southeastern USA is characterized by isoprene concentrations and low to modest NO_x emissions outside of urban areas. The sampling location is a rural site with low average NO_x concentrations (Lee et al., 2016; Edwards et al., 2017). The profile of $C_4H_7NO_5$ showed a clear peak during daytime with high variability. Finally, in central Amazonia, Brazil there was a strong daytime peak. The location is remote from anthropogenic sources, exhibiting very low NO_x concentrations (average = 0.62 ppb), and consequently lower $C_4H_7NO_5$ compared to the other isoprene-rich areas, Hong Kong with much higher NO_x (average = 5 ppb) and southeastern USA with slightly higher NO_x levels (average = 0.67 ppb).

The dominant role of $C_4H_7NO_5$ observed during nighttime in ambient measurements could be due to lack of major losses by NO_3 and O_3 leading to efficient accumulation as well as from air mass aging processes. A few plausible reactions forming $C_4H_7NO_5$ isomers during nighttime have been discussed in Paper V and the most significant ones have been added in the updated FZJ-NO_3-Isoprene mechanism (Vereecken et al., 2021) to test the potential contribution to $C_4H_7NO_5$ production during the

SAPHIR experiments. FZJ-NO_3-Isoprene mechanism is based on the MCMv3.3.1 (Jenkin et al., 1997; Saunders et al., 2003; Jenkin et al., 2015) and includes the more explicit descriptions from the CalTech mechanism (Wennberg et al., 2018). The predicted concentration profiles compared to the I-CIMS measurements, however, there was a significant discrepancy in the absolute concentrations. This discrepancy could be due to unknown formation pathways, such as decomposition of epoxides and peroxides formed by the NO_3-initiated oxidation of isoprene and highlighted as major contributing species in the model ((Vereecken et al., 2021). It is unclear if produced epoxides and peroxides are unstable and can decompose into C_4 products ($C_4H_7NO_5$ being one of them) in the gas phase or on available surfaces, thus explaining why only low concentration of these were observed. However, this chemistry is not well-known and needs further attention.

4.3 Aerosol formation from N-containing compounds

The role of NO_x on new particle formation (NPF) during the OH oxidation of TMB (Paper I) as well as the gas-to-particle partitioning of isoprene-derived organonitrates under different types of aerosol seeds and loading will be discussed in this section.

4.3.1 Nucleation and NPF supression

NO_x addition had a significant influence on the new particle formation during the TMB oxidation experiments. The NO_x effect can be understood by the comparison of the major cause behind NPF in the NO_x-free and NO_x-containing experiments.

In the NO_x-free oxidation experiments of TMB significant new particle formation was observed when applying the highest OH exposure (experiment 4 and to some extend experiment 3, table 4.1). On the other hand, there was no NPF when applying only modest OH exposures. It has been shown that dimers can play an important role on NPF (Ehn et al., 2014; Tröstl et al., 2016; Mohr et al., 2017; McFiggans et al., 2019), by having low enough volatility to initiate NPF. As it has

been discussed in section 4.1.1 higher OH exposures enhance dimer formation. Thus, sufficient levels of OH radicals are essential in order to facilitate dimer formation creating concentration levels that provide critical nucleus formation and initiate NPF. Dimer contribution was the highest in experiment 3 and slightly lower in experiment 4 even though it had a higher OH exposure. The lower dimer contribution in experiment 4 can be explained by the substantial NPF, and consequently large surface area that can lead to loss of dimers due to condensation sink. Similar behavior where dimers from biogenic precursors had lower contribution during NPF events compared to periods without NPF was observed in a boreal forest (Mohr et al., 2017). Apart from the OH exposure effect on NPF during TMB oxidation, (Li et al., 2021) recently showed that oxidation of a mixture of TMB with n-dodecane enhance SOA formation.

New particle formation was not occurred whenever the nitrated compounds had the highest contribution. Only in the NO_x1 experiment a reduced particle formation was observed, but in that case the HOM monomers and dimers were the dominant products. Dimer formation was drastically reduced in the presence of elevated NOx whilst ONs contribution was increasing with increasing NO addition. This change on the product distribution was responsible for the suppression of NPF, as the produced nitrogen-containing compounds were more volatile compared to dimers thus limiting the occurrence of NPF from TMB oxidation. A similar observation on suppression of NPF from monoterpene oxidation has been reported by (Wildt et al., 2014; Lehtipalo et al., 2018).

4.3.2 Partitioning of ONs from isoprene oxidation – Effect of neutral and acidic seeds

In Paper III the saturation vapor pressures of isoprene-derived ONs were estimated (figure 4.5). According to these estimations, the products with the highest propensity to condense were the 2N and especially 3N-dimers, as their volatilities ranged from SVOC to ELVOC. The 2N and 3N-monomers volatilities spanned from IVOC to LVOC with most of them falling in the SVOC class, meaning that 2N and 3N-monomers can condense in significant fractions if the organic mass loading is in the range of 1 – 10 μg m^{-3}. Finally, the 1N-monomers were the most volatile as they were mostly in the IVOC class with some of them being SVOC.

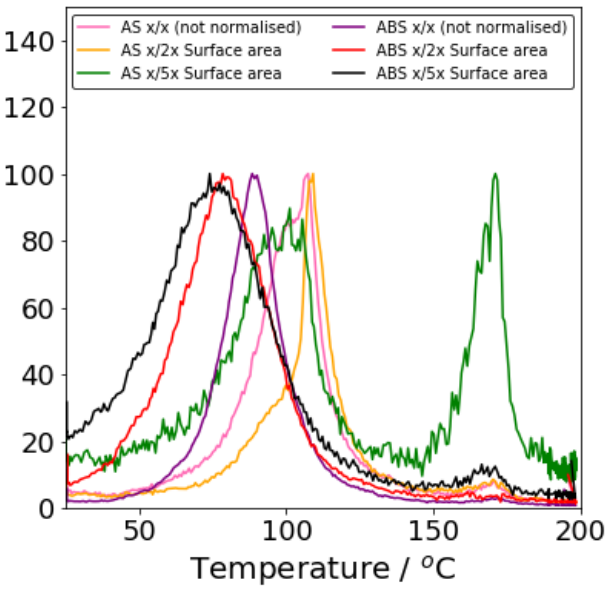

Figure 4.9: The normalized desorption profiles of $C_5H_8N_2O_8$ using ammonium sulfate (AS) or ammonium bisulfate (ABS) as seeds in three different aerosol mass loadings. Pink, yellow and green represent the AS experiments while purple, red and black represent the ABS ones.

The effects of mass loadings and surface areas on partitioning of selected nitrogen-containing products were studied using experiments with added neutral or acidic seed particles. The isoprene products were produced by NO_3-initiated oxidation using the Go:PAM flow reactor where the product distribution was monitored using the FIGAERO-CIMS. A list of the experiments is given in table 4.3 The experiments were classified into neutral or acidic depending on the added seeds of ammonium sulfate (AS) or ammonium bisulfate (ABS), respectively, and the seed mass loading denoted as x, 2x and 5x. Furthermore, the experiments can be divided into oxidant or VOC dominant regime depending on the initial concentrations of isoprene and NO_3. The signals of ions were corrected for background, normalized to the sum of $I^-$and H_2OI^- at 10^6 counts per second as well as to the average seed surface area due to different mass loadings.

In general, 1N, 2N, and 3N-monomers and 2N and 3N-accretion products (here named as "dimers") were identified in both gas and particle phase. The dominant products in the particle phase were $C_5H_8N_2O_8$ and $C_5H_{10}N_2O_8$. The 2N-dimers had weak contributions with $C_{10}H_{16}N_2O_{11}$ having the clearest desorption profile. Among the 3N-dimers $C_{10}H_{17}N_3O_{12,13}$ contributed more than the 2N-dimers, while

the rest of the 3N-Dimers had very weak signals. On the other hand, the secondary 1N-monomer $C_5H_9NO_7$ and the secondary fragmentation product propanonitrate ($C_3H_5NO_4$) had significant contributions. The low yield of 2N and 3N-dimers in the condensed phase might be explained by the relatively short residence time.

To understand the desorption process a screening of the desorption behavior for all

Table 4.3: List of experiments and summary of experimental conditions. AS=Ammonium sulfate, ABS=Ammonium bisulfate.

Exp.	Conditions	dominant chem. regime	$[Isoprene]_0$ (ppb)	$[N_2O_5]_0$ (ppb)	Type of seeds	Seed mass loading (µg m^{-3})	Seed surface area (nm^2 cm^{-3})
1	5x	Ox.	17	19	AS	84	$3.7x10^9$
2	2x	Ox.	17	19	AS	50	$2.6x10^9$
3	x	Ox.	17	19	AS	16	$1.0x10^9$
4	5x	Ox.	17	19	ABS	150	$6.5x10^9$
5	2x	Ox.	17	19	ABS	47	$2.4x10^9$
6	x	Ox.	17	19	ABS	27	$1.6x10^9$
7	5x	VOC	27	19	AS	91	$4.0x10^9$
8	2x	VOC	27	19	ABS	140	$5.8x10^9$
9	x	VOC	27	19	ABS	18	$1.1x10^9$
10	5x	VOC	27	19	AS	88	$4.0x10^9$

masses at unit mass resolution was done. For most of the nominal masses there were a prominent desorption maxima at very high temperature, above 180 ° C. This could be the result of ELVOCs or fragments from such compounds. However, since the feature were found at most m/z it was attributed to a matrix effect resulting from evaporation/decomposition of the seed particles with subsequent ionization and detection of co-evaporating organics. To scrutinize this further the desorption profile of the specific compounds was characterized. Many of these had multiple peaks where one (at high T) could be assigned to the matrix effect while the other was assumed to be the actual evaporation of the organic compounds. The first T_{max} of the measured products ranged from less than 30 to 120 °C (figure 4.10). The particle to gas ratio of the measured ONs in logarithmic scale during the

neutral and acidic seeded experiments did not show a clear increase for different conditions. This could be related to the short residence time and that partitioning did not establish on that time scale. However, it is clear that there was a general shift in T_{max} when ABS seeds were used compared to AS seeds. (figure 4.9). The ONs tended to have higher T_{max} when AS seeds were used while there was a shift of the desorption peak to lower temperatures with ABS seeds.

Another observation on the T_{max} was an effect due to the mass loading. The desorption peak during the experiment with the lowest mass loading (denoted as x) of ABS was at a higher temperature compared to the higher mass loading experiments of ABS but at a lower temperature compared to the AS experiments. This difference can be due to gradual neutralization of the acidic seeds during the oxidation process. Finally, as it was expected the particle fraction of the measured ONs increased with increasing molecular mass (figure 4.11). In general, compounds with higher mass have the propensity to be low volatile products and can contain more functional groups that also can decrease further the volatility of a compound.

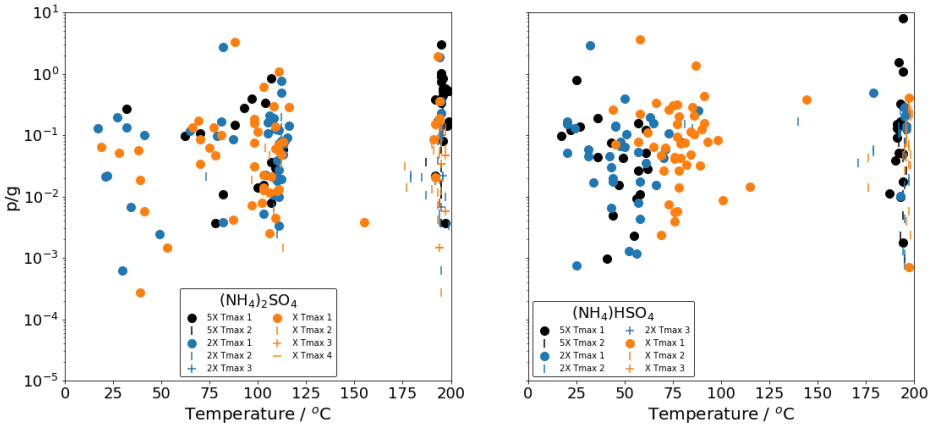

Figure 4.10: Particle to gas (p/g) versus T_{max} for identified ONs using either AS seeds (left) or ABS seeds (right) under three different mass loadings.

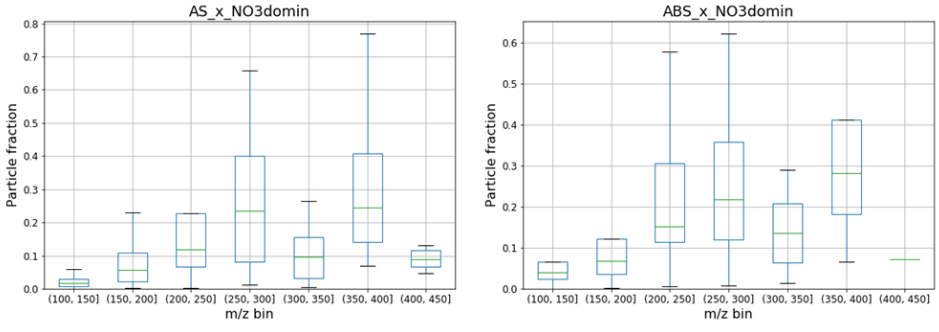

Figure 4.11: Particle fraction of produced ONs. The ONs are lumped into bins according to their molecular mass (m/z).

5

Concluding remarks – Atmospheric implications

This work focuses on laboratory studies on formation and fate of nitrogen-containing products from OH-initiated oxidation of TMB under different conditions and NO_3-initiated oxidation of isoprene. Ambient observations of isoprene-derived organonitrates (ONs) have been used to interpret the experimental data while the ambient measurements of nitro-aromatics were used to quantify various sources to ambient concentration profiles.

The identified ON products from TMB and isoprene oxidation can be used as tracers during ambient observations to classify sources into anthropogenic and biogenic. The characterized oxidation products families from TMB as well as the time behavior of the isoprene nitrate groups of 1N, 2N, and 3N-monomers and 2N and 3N-dimers can indicate the stage of aging processes and be used in clustering methods and for further source apportionment (Massoli et al., 2018; Xu et al., 2021; Ye et al., 2021; Mehra et al., 2021). In addition, nitrophenol and its analogues are good tracers of biomass burning (BB) but are also important products from secondary chemistry.

The N-containing products can act as NO_x reservoir and/or as permanent sink affecting the NO_x and NO_y budget in the atmosphere and consequently ozone formation. The oxidation experiments of TMB showed that the OH exposure and initial NO_x : VOC ratio are changing the monomers-dimers distribution of highly oxygenated organic molecules (HOM). In general, with increasing OH exposure and increased likelihood of a second OH attack, a higher contribution from second-generation oxidation products and dimers was observed. The enhancement in dimer formation is attributed to the increased RO_2 concentrations from the increased and fast TMB consumption by OH. The addition of NO_x to simulate urban conditions leads to the formation of ONs in addition to HOM. The formation and relative contribution of ON is increasing with increasing NO_x : ΔTMB ratio, mostly at the expense of dimers. This is a result of the competition of the reaction of HOM-RO_2 + NO with the HOM-RO_2 self-reaction, yielding primarily a reduction in dimer formation.

Alkyl nitrate (AN) molar yield from NO_3 + isoprene is found to be (108 $\pm$ 15)% during the experiments in SAPHIR chamber, suggesting that the amounts of ONs formed from NO_3-initiated oxidation of isoprene can be significant. The identified isoprene 1N, 2N, and 3N-monomers and 2N- and 3N-dimers characterized by different time behaviors, indicating the occurrence of multi-generation oxidation during the experiments. Ambient observations at different sampling sites showed

that the isoprene-derived ON from secondary chemistry with the chemical formula $C_4H_7NO_5$ was the dominant product measured both during daytime and nighttime. This highlights the importance of multi-generation formation pathways in ambient chemical conditions, suggesting that the understanding of these secondary processes is necessary to better describe aging processes of products from NO_3-initiated oxidation of isoprene as well as the effects of these nighttime products to the initiation of tropospheric ozone formation during the following day in areas with high biogenic emissions (Schwantes et al., 2020).

New particle formation (NPF) was observed during OH-initiated oxidation experiments of TMB. The experiments with the highest OH exposures led to particle formation when NO_x was not added since the dimer contribution was significant under these conditions and dimers are important for NPF. The product distribution changed with elevated NO_x concentrations leading to formation of ONs and suppression of dimers formation, and subsequently NPF. As a result, the interpretation of NPF from aromatics in urban areas should particularly consider the OH exposure, NO_x levels and RO_2 concentrations in detail since they largely determine the formation of ONs and consequently regulates NPF. Recent ambient measurements highlighted the decisive role of NO_x in formation of oxygenated organic molecules from both anthropogenic and biogenic precursors that can participate in secondary organic aerosol (SOA) formation in densely populated areas (Liu et al., 2021) .

The oxidation experiments of isoprene + NO_3 in the SAPHIR chamber enabled the measurement of a bulk organonitrate SOA mass yield of 3 to 6% and a bulk combined organic and organonitrate SOA mass yield of 13 to 15%. Furthermore, a SOA mass yield of about 5% ± 2% was estimated taking in consideration the assumption that only the dimers in the LVOC or ELVOC range will condense onto particles completely. This value represents a lower limit as SVOC species can also partition under higher mass loadings. These SOA mass yields are lower compared to SOA mass yields of other systems, e.g. photo-oxidation of monoterpenes. However, the large isoprene emissions indicate that the isoprene-derived ONs can produce significant amounts of SOA globally. Finally, the seeded experiments in the Go:PAM flow reactor showed that apart from 2N and 3N dimers, the monomers with 2N and 3N as well as some 1N secondary monomers do participate in the particle phase while the type of seeds, neutral or acidic, can play a role on changing the physicochemical properties of the partitioning products.

6

Future perspectives

A few ideas and open questions will be briefly discussed based on the results presented in this thesis.

Aromatics like TMB can form highly oxygenated organic molecules (HOM) monomers and dimers leading to NPF in NO_x-free and unseeded conditions. The addition of NO_x results to formation of ONs and suppression of dimers and consequently NPF, meaning that the formed ONs are more volatile compared to dimers. However, the produced ONs can still have low enough volatilities that enables the partitioning in the presence of aerosol loadings especially in polluted urban areas. Thus, the description of aromatics chemistry in urban areas should be considered in atmospheric models, as their representation has been neglected or highly simplified in current global atmospheric models (Taraborrelli et al., 2021).

The isoprene-derived ON $C_4H_7NO_5$ was a dominant species in the ambient observations during both daytime and nighttime while the chamber experiments showed that it does not have any strong sinks. This suggests that $C_4H_7NO_5$ isoprene ONs could be important as a long-term organic reservoir species of NO_x, in comparison to the other more reactive isoprene-derived ONs, affecting the formation of ozone. Thus, further understanding of the distribution of $C_4H_7NO_5$ isomers and their specific chemistry, and especially, a focus on the predicted dominant product family of the nitrated epoxides (Vereecken et al., 2021), whose secondary chemistry and therefore potential for forming $C_4H_7NO_5$ is largely unknown, is a necessity.

The neutral and acidic seeded experiments of NO_3-initiated oxidation of isoprene showed that the mass loading and the pH of the seeds can change the properties, e.g. T_{max}, of the products partitioning between the gas and particle phase. Further surface interaction studies are needed to provide more insights into this behavior.

Acknowledgements

I am grateful that during this long journey I met and worked with many people from around the world. This experience is invaluable!

First of all, I would like to acknowledge my supervisor **Professor Mattias Hallquist** for giving me the opportunity to do this thesis with him. His support and kindness were very helpful through this long process. I would also like to thank my co-supervisors **PD Dr. Thomas Mentel** for fruitful discussions and support during my visits in Forschungszentrum in Jülich and **Dr. Christian Mark Salvador** with whom I was sharing the office for four years, for our everyday conversations and for always helping me with ChemDraw. I also thank my examiner **Professor Jan Pettersson** for always asking me motivating questions.

I would like to thank the collaborators, especially **Hendrik, Anna, Rongrong and Sungah**, for creating a productive and friendly environment during the campaigns in Forschungszentrum in Jülich. Also, I want to thank **Professor Joel Thornton** for letting me spend time in his lab in University of Washington as well as **Ben** and **Brett** for their help during the experiments. Many thanks to all my **co-authors** for insightful comments and questions. The research presented is a contribution to the Swedish strategic research area ModElling the Regional and Global Earth system (MERGE) and supported by the Vetenskapsrådet (grant no. 2014-05332, 2013-06917 and 2018-04430), the Svenska Forskningsrådet Formas (grant no. 2015-1537 and 2019-586), the European Research Council (ERC) (SARLEP grant no. 681529) and European Commision (EC) under the European Union's Horizon 2020 research and innovation program (Eurochamp 2020 grant no. 730997 and FORCeS grant no. 821205). Åforsk, Adlerbertska Stipendiestiftelsen and Early Career Scientists (ECS) bursary by NOSA-FAAR 2018 were acknowledged for generous travel grants.

During my PhD I was part of the ClimBEco Graduate Research School and Mentoring Programme where I met a few other PhD students sharing the same thoughts and problems during our PhD journey. Cheers to all of you. I want also to express my gratitude to **Dr. Julia Grönros** for sharing her time to discuss research and private matters and giving me advice on how to navigate in the academic world.

Special thanks to the whole **Atmospheric Science Division** with its current and former members. I am really happy that apart from colleagues I also made friends. **Luis** and **Mike**, pals, thanks for your everyday discussions from scientific,

career and politics issues to music, films and philosophical matters in the coffee room or in a pub with some beer consumption. Luis, thanks for the help with the cover and being my climbing buddy. By the way, you need to train harder ☺! Mike, thanks for your great help during the final stages of my PhD. Thanks to **Julia** for guiding me the first days when I joined the group and for her great help with LaTeX. Thanks to **Emeritus Professor Johan Boman** for always being helpful and to **Senior Lecturer Erik Thomson** for always being friendly and talkative in the office especially during the silent pandemic times. **Sofia, Anna, Dimitri** to name some of you, thanks for creating a great working environment. Finally, thanks to all friends from the world outside of academia.

Την αγάπη μου στους γονείς μου και στα αδέρφια μου για την πολύπλευρη στήριξη όλα αυτά τα χρόνια!

References

Air quality in Europe 2021 (Feb. 26, 2022). URL: https://www.eea.europa.eu/publications/air-quality-in-europe-2021.

Albrecht, S. R. et al. (2019). "Measurements of hydroperoxy radicals (HO2) at atmospheric concentrations using bromide chemical ionisation mass spectrometry". In: *Atmos. Meas. Tech.* 12.2, pp. 891–902.

Aljawhary, D., A. K. Y. Lee, and J. P. D. Abbatt (2013). "High-resolution chemical ionization mass spectrometry (ToF-CIMS): application to study SOA composition and processing". In: *Atmospheric Measurement Techniques* 6.11, pp. 3211–3224.

Alsved, Malin et al. (2019). "Sources of Airborne Norovirus in Hospital Outbreaks". In: *Clinical Infectious Diseases* 70.10, pp. 2023–2028.

Arias, Paola et al. (2021). "Climate Change 2021: The Physical Science Basis. Contribution of Working Group14 I to the Sixth Assessment Report of the Intergovernmental Panel on Climate Change; Technical Summary". In.

Atkinson, R. and J. Arey (2003). "Gas-phase tropospheric chemistry of biogenic volatile organic compounds: a review". In: *Atmospheric Environment* 37, S197–S219.

Atkinson, R. et al. (2006). "Evaluated kinetic and photochemical data for atmospheric chemistry: Volume II andndash; gas phase reactions of organic species". In: *Atmos. Chem. Phys.* 6.11, pp. 3625–4055.

Bannan, T. J. et al. (2019). "A method for extracting calibrated volatility information from the FIGAERO-HR-ToF-CIMS and its experimental application". In: *Atmos. Meas. Tech.* 12.3, pp. 1429–1439.

Bannan, Thomas J. et al. (2015). "The first UK measurements of nitryl chloride using a chemical ionization mass spectrometer in central London in the summer of 2012, and an investigation of the role of Cl atom oxidation". In: *Journal of Geophysical Research: Atmospheres* 120.11, pp. 5638–5657.

Barsanti, Kelley C., Jesse H. Kroll, and Joel A. Thornton (2017). "Formation of Low-Volatility Organic Compounds in the Atmosphere: Recent Advancements and Insights". In: *The Journal of Physical Chemistry Letters* 8.7, pp. 1503–1511.

Bates, K. H. et al. (2021). "Development and evaluation of a new compact mechanism for aromatic oxidation in atmospheric models". In: *Atmos. Chem. Phys.* 21.24, pp. 18351–18374.

Beaver, M. R. et al. (2012). “Importance of biogenic precursors to the budget of organic nitrates: observations of multifunctional organic nitrates by CIMS and TD-LIF during BEARPEX 2009”. In: *Atmos. Chem. Phys.* 12.13, pp. 5773–5785.

Berndt, Torsten et al. (2016). “Hydroxyl radical-induced formation of highly oxidized organic compounds”. In: *Nature Communications* 7.1, p. 13677.

Berndt, Torsten et al. (2018). “Accretion Product Formation from Self- and Cross-Reactions of RO2 Radicals in the Atmosphere”. In: *Angewandte Chemie International Edition* 57.14, pp. 3820–3824.

Bertram, T. H. et al. (2011). “A field-deployable, chemical ionization time-of-flight mass spectrometer”. In: *Atmospheric Measurement Techniques* 4.7, pp. 1471–1479.

Bi, C. et al. (2021). “Quantification of isomer-resolved iodide chemical ionization mass spectrometry sensitivity and uncertainty using a voltage-scanning approach”. In: *Atmos. Meas. Tech.* 14.10, pp. 6835–6850.

Bianchi, F. et al. (2016). “New particle formation in the free troposphere: A question of chemistry and timing”. In: *Science* 352.6289, pp. 1109–1112.

Bianchi, Federico et al. (2019). “Highly Oxygenated Organic Molecules (HOM) from Gas-Phase Autoxidation Involving Peroxy Radicals: A Key Contributor to Atmospheric Aerosol”. In: *Chemical Reviews* 119.6, pp. 3472–3509.

Bloss, C. et al. (2005). “Development of a detailed chemical mechanism (MCMv3.1) for the atmospheric oxidation of aromatic hydrocarbons”. In: *Atmos. Chem. Phys.* 5.3, pp. 641–664.

Brean, J. et al. (2019). “Observations of highly oxidized molecules and particle nucleation in the atmosphere of Beijing”. In: *Atmos. Chem. Phys.* 19.23, pp. 14933–14947.

Brophy, P. and D. K. Farmer (2016). “Clustering, methodology, and mechanistic insights into acetate chemical ionization using high-resolution time-of-flight mass spectrometry”. In: *Atmos. Meas. Tech.* 9.8, pp. 3969–3986.

Brown, S. S. and J. Stutz (2012). “Nighttime radical observations and chemistry”. In: *Chem Soc Rev* 41.19, pp. 6405–47.

Brownwood, Bellamy et al. (2021). “Gas-Particle Partitioning and SOA Yields of Organonitrate Products from NO3-Initiated Oxidation of Isoprene under Varied Chemical Regimes”. In: *ACS Earth and Space Chemistry*.

Cabrera-Perez, D. et al. (2016). “Global atmospheric budget of simple monocyclic aromatic compounds”. In: *Atmos. Chem. Phys.* 16.11, pp. 6931–6947.

Calvert, Jack G et al. (2002). “The mechanisms of atmospheric oxidation of the aromatic hydrocarbons”. In.

Carlton, A. G., C. Wiedinmyer, and J. H. Kroll (2009). "A review of Secondary Organic Aerosol (SOA) formation from isoprene". In: *Atmospheric Chemistry and Physics* 9.14, pp. 4987–5005.

Cheng, X. et al. (2021). "Highly oxygenated organic molecules produced by the oxidation of benzene and toluene in a wide range of OH exposure and NOx conditions". In: *Atmos. Chem. Phys.* 21.15, pp. 12005–12019.

Claflin, M. S. et al. (2021). "An in situ gas chromatograph with automatic detector switching between PTR- and EI-TOF-MS: isomer-resolved measurements of indoor air". In: *Atmos. Meas. Tech.* 14.1, pp. 133–152.

Compernolle, S., K. Ceulemans, and J. F. Müller (2011). "EVAPORATION: a new vapour pressure estimation methodfor organic molecules including non-additivity and intramolecular interactions". In: *Atmos. Chem. Phys.* 11.18, pp. 9431–9450.

Crounse, J. D. et al. (2013). "Autoxidation of Organic Compounds in the Atmosphere". In: *Journal of Physical Chemistry Letters* 4.20, pp. 3513–3520.

Crounse, John D. et al. (2006). "Measurement of Gas-Phase Hydroperoxides by Chemical Ionization Mass Spectrometry". In: *Analytical Chemistry* 78.19, pp. 6726–6732.

Daellenbach, Kaspar R. et al. (2020). "Sources of particulate-matter air pollution and its oxidative potential in Europe". In: *Nature* 587.7834, pp. 414–419.

D'Ambro, E. L. et al. (2019). "Chamber-based insights into the factors controlling epoxydiol (IEPOX) secondary organic aerosol (SOA) yield, composition, and volatility". In: *Atmos. Chem. Phys.* 19.17, pp. 11253–11265.

Dockery, Douglas W and C Arden Pope (1994). "Acute respiratory effects of particulate air pollution". In: *Annual review of public health* 15.1, pp. 107–132.

Dockery, Douglas W. et al. (1993). "An Association between Air Pollution and Mortality in Six U.S. Cities". In: *New England Journal of Medicine* 329.24, pp. 1753–1759.

Donahue, N. M. et al. (2006). "Coupled Partitioning, Dilution, and Chemical Aging of Semivolatile Organics". In: *Environmental Science and Technology* 40.8, pp. 2635–2643.

Donahue, N. M. et al. (2011). "A two-dimensional volatility basis set: 1. organic-aerosol mixing thermodynamics". In: *Atmospheric Chemistry and Physics* 11.7, pp. 3303–3318.

Donahue, N. M. et al. (2012). "A two-dimensional volatility basis set – Part 2: Diagnostics of organic-aerosol evolution". In: *Atmospheric Chemistry and Physics* 12.2, pp. 615–634.

Donahue, Neil M., Allen L. Robinson, and Spyros N. Pandis (2009). "Atmospheric organic particulate matter: From smoke to secondary organic aerosol". In: *Atmospheric Environment* 43.1, pp. 94–106.

Edwards, P. M. et al. (2017). "Transition from high- to low-NOx control of night-time oxidation in the southeastern US". In: *Nature Geoscience* 10.7, pp. 490–495.

Ehn, M. et al. (2010). "Composition and temporal behavior of ambient ions in the boreal forest". In: *Atmos. Chem. Phys.* 10.17, pp. 8513–8530.

Ehn, M. et al. (2012). "Gas phase formation of extremely oxidized pinene reaction products in chamber and ambient air". In: *Atmos. Chem. Phys.* 12.11, pp. 5113–5127.

Ehn, M. et al. (2014). "A large source of low-volatility secondary organic aerosol". In: *Nature* 506.7489, pp. 476–9.

Eisele, F. L. and D. J. Tanner (1993). "Measurement of the gas phase concentration of H2SO4and methane sulfonic acid and estimates of H2SO4production and loss in the atmosphere". In: *Journal of Geophysical Research: Atmospheres* 98.D5, pp. 9001–9010.

Farman, J. C., B. G. Gardiner, and J. D. Shanklin (1985). "Large losses of total ozone in Antarctica reveal seasonal ClOx/NOx interaction". In: *Nature* 315.6016, pp. 207–210.

Faxon, C. et al. (2018). "Characterization of organic nitrate constituents of secondary organic aerosol (SOA) from nitrate-radical-initiated oxidation of limonene using high-resolution chemical ionization mass spectrometry". In: *Atmos. Chem. Phys.* 18.8, pp. 5467–5481.

Finlayson-Pitts, B. J. and J. N. Pitts (1999). *Chemistry of the Upper and Lower Atmosphere*.

Fowler, D. et al. (2020). "A chronology of global air quality". In: *Philos Trans A Math Phys Eng Sci* 378.2183, p. 20190314.

Frege, C. et al. (2017). "Chemical characterization of atmospheric ions at the high altitude research station Jungfraujoch (Switzerland)". In: *Atmospheric Chemistry and Physics* 17.4, pp. 2613–2629.

Fu, X. et al. (2019). "The significant contribution of HONO to secondary pollutants during a severe winter pollution event in southern China". In: *Atmos. Chem. Phys.* 19.1, pp. 1–14.

Fuchs, H. et al. (2012). "Comparison of N₂O₅ mixing ratios during NO3Comp 2007 in SAPHIR". In: *Atmos. Meas. Tech.* 5.11, pp. 2763–2777.

Fuchs, H. et al. (2017). “Comparison of OH reactivity measurements in the atmospheric simulation chamber SAPHIR”. In: *Atmos. Meas. Tech.* 10.10, pp. 4023–4053.

Fuzzi, S. et al. (2015). “Particulate matter, air quality and climate: lessons learned and future needs”. In: *Atmos. Chem. Phys.* 15.14, pp. 8217–8299.

Garmash, O. et al. (2020). “Multi-generation OH oxidation as a source for highly oxygenated organic molecules from aromatics”. In: *Atmos. Chem. Phys.* 20.1, pp. 515–537.

Gentner, Drew R. et al. (2017). “Review of Urban Secondary Organic Aerosol Formation from Gasoline and Diesel Motor Vehicle Emissions”. In: *Environmental Science and Technology* 51.3, pp. 1074–1093.

George, C. et al. (2015). “Heterogeneous photochemistry in the atmosphere”. In: *Chem Rev* 115.10, pp. 4218–58.

Glasius, Marianne and Allen H. Goldstein (2016). “Recent Discoveries and Future Challenges in Atmospheric Organic Chemistry”. In: *Environmental Science and Technology* 50.6, pp. 2754–2764.

Glasius, Marianne et al. (2021). “Chemical characteristics and sources of organosulfates, organosulfonates, and carboxylic acids in aerosols in urban Xi’an, Northwest China”. In: *Science of The Total Environment*, p. 151187.

Guenther, A. et al. (1995). “A Global-Model of Natural Volatile Organic-Compound Emissions”. In: *Journal of Geophysical Research-Atmospheres* 100.D5, pp. 8873–8892.

Guenther, A. B. et al. (2012). “The Model of Emissions of Gases and Aerosols from Nature version 2.1 (MEGAN2.1): an extended and updated framework for modeling biogenic emissions”. In: *Geosci. Model Dev.* 5.6, pp. 1471–1492.

Hakola, H. et al. (2012). “In situ measurements of volatile organic compounds in a boreal forest”. In: *Atmospheric Chemistry and Physics* 12.23, pp. 11665–11678.

Hallquist, M. et al. (2009). “The formation, properties and impact of secondary organic aerosol: current and emerging issues”. In: *Atmospheric Chemistry and Physics* 9.14, pp. 5155–5236.

Hallquist, Mattias et al. (2000). “Hydrolysis of N2O5 on Submicron Sulfuric Acid Aerosols”. In: *The Journal of Physical Chemistry A* 104.17, pp. 3984–3990.

Hamilton, Jacqueline F. et al. (2021). “Key Role of NO3 Radicals in the Production of Isoprene Nitrates and Nitrooxyorganosulfates in Beijing”. In: *Environmental Science and Technology*.

Hammes, J. et al. (2019). “Carboxylic acids from limonene oxidation by ozone and hydroxyl radicals: insights into mechanisms derived using a FIGAERO-CIMS”. In: *Atmos. Chem. Phys.* 19.20, pp. 13037–13052.

Heinritzi, M. et al. (2020). “Molecular understanding of the suppression of new-particle formation by isoprene”. In: *Atmos. Chem. Phys.* 20.20, pp. 11809–11821.

Henze, D. K. et al. (2008). “Global modeling of secondary organic aerosol formation from aromatic hydrocarbons: high- vs. low-yield pathways”. In: *Atmos. Chem. Phys.* 8.9, pp. 2405–2420.

Hinds, William C (1999). *Aerosol technology, second edition.* BMJ Publishing Group Ltd.

Huey, L. Gregory (2007). “Measurement of trace atmospheric species by chemical ionization mass spectrometry: Speciation of reactive nitrogen and future directions”. In: *Mass Spectrometry Reviews* 26.2, pp. 166–184.

Isaacman-VanWertz, G. et al. (2017). “Using advanced mass spectrometry techniques to fully characterize atmospheric organic carbon: current capabilities and remaining gaps”. In: *Faraday Discussions* 200.0, pp. 579–598.

Isaacman-VanWertz, Gabriel et al. (2018). “Chemical evolution of atmospheric organic carbon over multiple generations of oxidation”. In: *Nature Chemistry* 10.4, pp. 462–468.

Iyer, S. et al. (2016). “Modeling the Detection of Organic and Inorganic Compounds Using Iodide-Based Chemical Ionization”. In: *J Phys Chem A* 120.4, pp. 576–87.

Jenkin, M. E., J. C. Young, and A. R. Rickard (2015). “The MCM v3.3.1 degradation scheme for isoprene”. In: *Atmos. Chem. Phys.* 15.20, pp. 11433–11459.

Jenkin, M. E. et al. (2003). “Protocol for the development of the Master Chemical Mechanism, MCM v3 (Part B): tropospheric degradation of aromatic volatile organic compounds”. In: *Atmospheric Chemistry and Physics* 3.1, pp. 181–193.

Jenkin, Michael E., Sandra M. Saunders, and Michael J. Pilling (1997). “The tropospheric degradation of volatile organic compounds: a protocol for mechanism development”. In: *Atmospheric Environment* 31.1, pp. 81–104.

Ji, Y. et al. (2020). “A vacuum ultraviolet ion source (VUV-IS) for iodide–chemical ionization mass spectrometry: a substitute for radioactive ion sources”. In: *Atmos. Meas. Tech.* 13.7, pp. 3683–3696.

Jickells, T. et al. (2013). “The cycling of organic nitrogen through the atmosphere”. In: *Philos Trans R Soc Lond B Biol Sci* 368.1621, p. 20130115.

Jimenez, J. L. et al. (2009). “Evolution of organic aerosols in the atmosphere”. In: *Science* 326.5959, pp. 1525–9.

Jokinen, T. et al. (2012). “Atmospheric sulphuric acid and neutral cluster measurements using CI-APi-TOF”. In: *Atmospheric Chemistry and Physics* 12.9, pp. 4117–4125.

Jokinen, T. et al. (2014). “Rapid autoxidation forms highly oxidized RO2 radicals in the atmosphere”. In: *Angew Chem Int Ed Engl* 53.52, pp. 14596–600.

Jokinen, T. et al. (2015). “Production of extremely low volatile organic compounds from biogenic emissions: Measured yields and atmospheric implications”. In: *Proc Natl Acad Sci U S A* 112.23, pp. 7123–8.

Junninen, H. et al. (2010). “A high-resolution mass spectrometer to measure atmospheric ion composition”. In: *Atmospheric Measurement Techniques* 3.4, pp. 1039–1053.

Kanakidou, M. et al. (2005). “Organic aerosol and global climate modelling: a review”. In: *Atmospheric Chemistry and Physics* 5.4, pp. 1053–1123.

Kang, E. et al. (2007). “Introducing the concept of Potential Aerosol Mass (PAM)”. In: *Atmos. Chem. Phys.* 7.22, pp. 5727–5744.

Kiendler-Scharr, A. et al. (2016). “Ubiquity of organic nitrates from nighttime chemistry in the European submicron aerosol”. In: *Geophysical Research Letters* 43.14, pp. 7735–7744.

Kim, M. J. et al. (2016). “Revisiting benzene cluster cations for the chemical ionization of dimethyl sulfide and select volatile organic compounds”. In: *Atmospheric Measurement Techniques* 9.4, pp. 1473–1484.

Kleindienst, Tadeusz E. et al. (2007). “Ozone-isoprene reaction: Re-examination of the formation of secondary organic aerosol”. In: *Geophysical Research Letters* 34.1.

Koss, A. R. et al. (2016). “Evaluation of NO+ reagent ion chemistry for online measurements of atmospheric volatile organic compounds”. In: *Atmos. Meas. Tech.* 9.7, pp. 2909–2925.

Kostyukevich, Yury et al. (2018). “Hydrogen/deuterium exchange in mass spectrometry”. In: *Mass Spectrometry Reviews* 37.6, pp. 811–853.

Krechmer, J. E. et al. (2015). “Formation of Low Volatility Organic Compounds and Secondary Organic Aerosol from Isoprene Hydroxyhydroperoxide Low-NO Oxidation”. In: *Environ Sci Technol* 49.17, pp. 10330–9.

Krechmer, Jordan et al. (2018). “Evaluation of a New Reagent-Ion Source and Focusing Ion–Molecule Reactor for Use in Proton-Transfer-Reaction Mass Spectrometry”. In: *Analytical Chemistry* 90.20, pp. 12011–12018.

Kristensen, Kasper et al. (2016). “High-Molecular Weight Dimer Esters Are Major Products in Aerosols from alpha-Pinene Ozonolysis and the Boreal Forest”. In: *Environmental Science and Technology Letters* 3.8, pp. 280–285.

Kroll, J. H. and J. H. Seinfeld (2008). “Chemistry of secondary organic aerosol: Formation and evolution of low-volatility organics in the atmosphere”. In: *Atmospheric Environment* 42.16, pp. 3593–3624.

Kroll, J. H. et al. (2011). “Carbon oxidation state as a metric for describing the chemistry of atmospheric organic aerosol”. In: *Nat Chem* 3.2, pp. 133–9.

Kroll, Jesse H. et al. (2005). “Secondary organic aerosol formation from isoprene photooxidation under high-NOx conditions”. In: *Geophysical Research Letters* 32.18.

Kurtén, Theo et al. (2016). “alpha-Pinene Autoxidation Products May Not Have Extremely Low Saturation Vapor Pressures Despite High O:C Ratios”. In: *The Journal of Physical Chemistry A* 120.16, pp. 2569–2582.

Kürten, A. et al. (2016). “Observation of new particle formation and measurement of sulfuric acid, ammonia, amines and highly oxidized organic molecules at a rural site in central Germany”. In: *Atmos. Chem. Phys.* 16.19, pp. 12793–12813.

Kürten, Andreas et al. (2012). “Calibration of a Chemical Ionization Mass Spectrometer for the Measurement of Gaseous Sulfuric Acid”. In: *The Journal of Physical Chemistry A* 116.24, pp. 6375–6386.

Laskin, J., A. Laskin, and S. A. Nizkorodov (2018). “Mass Spectrometry Analysis in Atmospheric Chemistry”. In: *Anal Chem* 90.1, pp. 166–189.

Lavi, A. et al. (2018). “The sensitivity of benzene cluster cation chemical ionization mass spectrometry to select biogenic terpenes”. In: *Atmos. Meas. Tech.* 11.6, pp. 3251–3262.

Le Breton, M. et al. (2018a). “Chlorine oxidation of VOCs at a semi-rural site in Beijing: significant chlorine liberation from ClNO2 and subsequent gas- and particle-phase Cl–VOC production”. In: *Atmos. Chem. Phys.* 18.17, pp. 13013–13030.

Le Breton, M. et al. (2018b). “Online gas- and particle-phase measurements of organosulfates, organosulfonates and nitrooxy organosulfates in Beijing utilizing a FIGAERO ToF-CIMS”. In: *Atmos. Chem. Phys.* 18.14, pp. 10355–10371.

Le Breton, Michael et al. (2014a). “Simultaneous airborne nitric acid and formic acid measurements using a chemical ionization mass spectrometer around the UK: Analysis of primary and secondary production pathways”. In: *Atmospheric Environment* 83, pp. 166–175.

Le Breton, Michael et al. (2014b). “The first airborne comparison of N2O5 measurements over the UK using a CIMS and BBCEAS during the RONOCO campaign”. In: *Analytical Methods* 6.24, pp. 9731–9743.

Lee, B. H. et al. (2014). “An iodide-adduct high-resolution time-of-flight chemical-ionization mass spectrometer: application to atmospheric inorganic and organic compounds”. In: *Environ Sci Technol* 48.11, pp. 6309–17.

Lee, B. H. et al. (2016). “Highly functionalized organic nitrates in the southeast United States: Contribution to secondary organic aerosol and reactive nitrogen budgets”. In: *Proc Natl Acad Sci U S A* 113.6, pp. 1516–21.

Lehtipalo, Katrianne et al. (2018). “Multicomponent new particle formation from sulfuric acid, ammonia, and biogenic vapors”. In: *Science Advances* 4.12, eaau5363.

Lelieveld, J. et al. (2015). “The contribution of outdoor air pollution sources to premature mortality on a global scale”. In: *Nature* 525.7569, pp. 367–371.

Lelieveld, J. et al. (2016). “Global tropospheric hydroxyl distribution, budget and reactivity”. In: *Atmos. Chem. Phys.* 16.19, pp. 12477–12493.

Lelieveld, J. et al. (2019). “Effects of fossil fuel and total anthropogenic emission removal on public health and climate”. In: *Proceedings of the National Academy of Sciences* 116.15, pp. 7192–7197.

Li, H. et al. (2018). “Nitrate-driven urban haze pollution during summertime over the North China Plain”. In: *Atmos. Chem. Phys.* 18.8, pp. 5293–5306.

Li, J. et al. (2019a). “Verification of anthropogenic VOC emission inventory through ambient measurements and satellite retrievals”. In: *Atmos. Chem. Phys.* 19.9, pp. 5905–5921.

Li, J. et al. (2021). “Enhanced secondary organic aerosol formation from the photooxidation of mixed anthropogenic volatile organic compounds”. In: *Atmos. Chem. Phys.* 21.10, pp. 7773–7789.

Li, X. et al. (2019b). “Relative humidity effect on the formation of highly oxidized molecules and new particles during monoterpene oxidation”. In: *Atmos. Chem. Phys.* 19.3, pp. 1555–1570.

Liu, S. et al. (2021). “Synergetic effects of NH3 and NOx on the production and optical absorption of secondary organic aerosol formation from toluene photooxidation”. In: *Atmos. Chem. Phys.* 21.23, pp. 17759–17773.

Lopez-Hilfiker, F. D. et al. (2014). “A novel method for online analysis of gas and particle composition: description and evaluation of a Filter Inlet for Gases and AEROsols (FIGAERO)”. In: *Atmospheric Measurement Techniques* 7.4, pp. 983–1001.

Lopez-Hilfiker, F. D. et al. (2016). “Constraining the sensitivity of iodide adduct chemical ionization mass spectrometry to multifunctional organic molecules using the collision limit and thermodynamic stability of iodide ion adducts”. In: *Atmos. Meas. Tech.* 9.4, pp. 1505–1512.

Lopez-Hilfiker, F. D. et al. (2019). “An extractive electrospray ionization time-of-flight mass spectrometer (EESI-TOF) for online measurement of atmospheric aerosol particles”. In: *Atmos. Meas. Tech.* 12.9, pp. 4867–4886.

Loreto, Francesco et al. (2014). “Plant volatiles and the environment”. In: *Plant, Cell and Environment* 37.8, pp. 1905–1908.

Lutz, Anna et al. (2019). “Gas to Particle Partitioning of Organic Acids in the Boreal Atmosphere”. In: *ACS Earth and Space Chemistry* 3.7, pp. 1279–1287.

Massoli, Paola et al. (2018). “Ambient Measurements of Highly Oxidized Gas-Phase Molecules during the Southern Oxidant and Aerosol Study (SOAS) 2013”. In: *ACS Earth and Space Chemistry* 2.7, pp. 653–672.

McDonald, B. C. et al. (2018). “Volatile chemical products emerging as largest petrochemical source of urban organic emissions”. In: *Science* 359.6377, pp. 760–764.

McFiggans, Gordon et al. (2019). “Secondary organic aerosol reduced by mixture of atmospheric vapours”. In: *Nature* 565.7741, pp. 587–593.

Mehra, Archit et al. (2021). “Using highly time-resolved online mass spectrometry to examine biogenic and anthropogenic contributions to organic aerosol in Beijing”. In: *Faraday Discussions*.

Mentel, T. F. et al. (2015). “Formation of highly oxidized multifunctional compounds: autoxidation of peroxy radicals formed in the ozonolysis of alkenes – deduced from structure–product relationships”. In: *Atmospheric Chemistry and Physics* 15.12, pp. 6745–6765.

Mohr, C. et al. (2017). “Ambient observations of dimers from terpene oxidation in the gas phase: Implications for new particle formation and growth”. In: *Geophysical Research Letters* 44.6, pp. 2958–2966.

Mohr, Claudia et al. (2019). “Molecular identification of organic vapors driving atmospheric nanoparticle growth”. In: *Nature Communications* 10.1, p. 4442.

Molteni, U. et al. (2018). “Formation of highly oxygenated organic molecules from aromatic compounds”. In: *Atmospheric Chemistry and Physics* 18.3, pp. 1909–1921.

Molteni, Ugo et al. (2019). “Formation of Highly Oxygenated Organic Molecules from alpha-Pinene Ozonolysis: Chemical Characteristics, Mechanism, and Kinetic Model Development”. In: *ACS Earth and Space Chemistry* 3.5, pp. 873–883.

Müller, J. F., J. Peeters, and T. Stavrakou (2014). “Fast photolysis of carbonyl nitrates from isoprene”. In: *Atmos. Chem. Phys.* 14.5, pp. 2497–2508.

Müller, J. F. et al. (2008). “Global isoprene emissions estimated using MEGAN, ECMWF analyses and a detailed canopy environment model”. In: *Atmos. Chem. Phys.* 8.5, pp. 1329–1341.

Nannoolal, Yash, Jürgen Rarey, and Deresh Ramjugernath (2008). “Estimation of pure component properties: Part 3. Estimation of the vapor pressure of non-electrolyte organic compounds via group contributions and group interactions”. In: *Fluid Phase Equilibria* 269.1, pp. 117–133.

Nault, B. A. et al. (2021). “Secondary organic aerosols from anthropogenic volatile organic compounds contribute substantially to air pollution mortality”. In: *Atmos. Chem. Phys.* 21.14, pp. 11201–11224.

Ng, N. L. et al. (2007). “Secondary organic aerosol formation from m-xylene, toluene, and benzene”. In: *Atmos. Chem. Phys.* 7.14, pp. 3909–3922.

Ng, N. L. et al. (2017). “Nitrate radicals and biogenic volatile organic compounds: oxidation, mechanisms, and organic aerosol”. In: *Atmos. Chem. Phys.* 17.3, pp. 2103–2162.

Pankow, J. F. and W. E. Asher (2008). “SIMPOL.1: a simple group contribution method for predicting vapor pressures and enthalpies of vaporization of multifunctional organic compounds”. In: *Atmos. Chem. Phys.* 8.10, pp. 2773–2796.

Pankow, James F. (1994). “An absorption model of the gas/aerosol partitioning involved in the formation of secondary organic aerosol”. In: *Atmospheric Environment* 28.2, pp. 189–193.

Paulot, F., D. K. Henze, and P. O. Wennberg (2012). “Impact of the isoprene photochemical cascade on tropical ozone”. In: *Atmos. Chem. Phys.* 12.3, pp. 1307–1325.

Peeters, J., T. L. Nguyen, and L. Vereecken (2009). “HOx radical regeneration in the oxidation of isoprene”. In: *Phys Chem Chem Phys* 11.28, pp. 5935–9.

Peng, Xiang et al. (2022). “Photodissociation of particulate nitrate as a source of daytime tropospheric Cl2”. In: *Nature Communications* 13.1, p. 939.

Peräkylä, O. et al. (2020). “Experimental investigation into the volatilities of highly oxygenated organic molecules (HOMs)”. In: *Atmos. Chem. Phys.* 20.2, pp. 649–669.

Porter, W. C., S. A. Safieddine, and C. L. Heald (2017). “Impact of aromatics and monoterpenes on simulated tropospheric ozone and total OH reactivity”. In: *Atmospheric Environment* 169, pp. 250–257.

Priestley, M. et al. (2021). “Chemical characterisation of benzene oxidation products under high- and low-NOx conditions using chemical ionisation mass spectrometry”. In: *Atmos. Chem. Phys.* 21.5, pp. 3473–3490.

Pullinen, I. et al. (2020). “Impact of NOx on secondary organic aerosol (SOA) formation from alpha-pinene and beta-pinene photooxidation: the role of highly oxygenated organic nitrates”. In: *Atmos. Chem. Phys.* 20.17, pp. 10125–10147.

Pöschl, Ulrich and Manabu Shiraiwa (2015). “Multiphase Chemistry at the Atmosphere–Biosphere Interface Influencing Climate and Public Health in the Anthropocene”. In: *Chemical Reviews* 115.10, pp. 4440–4475.

Ran, Liang et al. (2009). “Ozone photochemical production in urban Shanghai, China: Analysis based on ground level observations”. In: *Journal of Geophysical Research: Atmospheres* 114.D15.

Riedel, Theran P. et al. (2012). “Nitryl Chloride and Molecular Chlorine in the Coastal Marine Boundary Layer”. In: *Environmental Science and Technology* 46.19, pp. 10463–10470.

Riipinen, I. et al. (2012). “The contribution of organics to atmospheric nanoparticle growth”. In: *Nature Geoscience* 5.7, pp. 453–458.

Rissanen, M. P. et al. (2019). “Multi-scheme chemical ionization inlet (MION) for fast switching of reagent ion chemistry in atmospheric pressure chemical ionization mass spectrometry (CIMS) applications”. In: *Atmos. Meas. Tech.* 12.12, pp. 6635–6646.

Rissanen, Matti (2021). “Anthropogenic Volatile Organic Compound (AVOC) Autoxidation as a Source of Highly Oxygenated Organic Molecules (HOM)”. In: *The Journal of Physical Chemistry A* 125.41, pp. 9027–9039.

Riva, M. et al. (2019). “Evaluating the performance of five different chemical ionization techniques for detecting gaseous oxygenated organic species”. In: *Atmos. Meas. Tech.* 12.4, pp. 2403–2421.

Rohrer, F. et al. (2005). “Characterisation of the photolytic HONO-source in the atmosphere simulation chamber SAPHIR”. In: *Atmos. Chem. Phys.* 5.8, pp. 2189–2201.

Salvador, C. M. G. et al. (2021). “Ambient nitro-aromatic compounds – biomass burning versus secondary formation in rural China”. In: *Atmos. Chem. Phys.* 21.3, pp. 1389–1406.

Sato, K. et al. (2012). “AMS and LC/MS analyses of SOA from the photooxidation of benzene and 1,3,5-trimethylbenzene in the presence of NOx: effects of chemical structure on SOA aging”. In: *Atmos. Chem. Phys.* 12.10, pp. 4667–4682.

Saunders, S. M. et al. (2003). “Protocol for the development of the Master Chemical Mechanism, MCM v3 (Part A): tropospheric degradation of non-aromatic volatile organic compounds”. In: *Atmos. Chem. Phys.* 3.1, pp. 161–180.

Schiestl, Florian P. (2010). “The evolution of floral scent and insect chemical communication”. In: *Ecology Letters* 13.5, pp. 643–656.

Schobesberger, S. et al. (2018). “A model framework to retrieve thermodynamic and kinetic properties of organic aerosol from composition-resolved thermal desorption measurements”. In: *Atmos. Chem. Phys.* 18.20, pp. 14757–14785.

Schwantes, R. H. et al. (2020). “Comprehensive isoprene and terpene gas-phase chemistry improves simulated surface ozone in the southeastern US”. In: *Atmos. Chem. Phys.* 20.6, pp. 3739–3776.

Seinfeld, J.H. and S.N. Pandis (2016). *Atmospheric Chemistry and Physics: From Air Pollution to Climate Change*. Wiley.

Sharkey, Thomas D., Amy E. Wiberley, and Autumn R. Donohue (2007). “Isoprene Emission from Plants: Why and How”. In: *Annals of Botany* 101.1, pp. 5–18.

Shrivastava, Manish et al. (2017). “Recent advances in understanding secondary organic aerosol: Implications for global climate forcing”. In: *Reviews of Geophysics* 55.2, pp. 509–559.

Sporre, M. K. et al. (2020). “Large difference in aerosol radiative effects from BVOC-SOA treatment in three Earth system models”. In: *Atmos. Chem. Phys.* 20.14, pp. 8953–8973.

Stark, H. et al. (2015). “Methods to extract molecular and bulk chemical information from series of complex mass spectra with limited mass resolution”. In: *International Journal of Mass Spectrometry* 389, pp. 26–38.

Tang, J. W. et al. (2021). “Dismantling myths on the airborne transmission of severe acute respiratory syndrome coronavirus-2 (SARS-CoV-2)”. In: *Journal of Hospital Infection* 110, pp. 89–96.

Taraborrelli, D. et al. (2021). “Influence of aromatics on tropospheric gas-phase composition”. In: *Atmos. Chem. Phys.* 21.4, pp. 2615–2636.

Thornton, Joel A. et al. (2020). “Evaluating Organic Aerosol Sources and Evolution with a Combined Molecular Composition and Volatility Framework Using the Filter Inlet for Gases and Aerosols (FIGAERO)”. In: *Accounts of Chemical Research* 53.8, pp. 1415–1426.

Tröstl, Jasmin et al. (2016). “The role of low-volatility organic compounds in initial particle growth in the atmosphere”. In: *Nature* 533.7604, pp. 527–531.

Tsigaridis, K. et al. (2014). “The AeroCom evaluation and intercomparison of organic aerosol in global models”. In: *Atmos. Chem. Phys.* 14.19, pp. 10845–10895.

Tsiligiannis, E. et al. (2019). “Effect of NOx on 1,3,5-trimethylbenzene (TMB) oxidation product distribution and particle formation”. In: *Atmos. Chem. Phys.* 19.23, pp. 15073–15086.

Tsiodra, I. et al. (2021). “Annual exposure to polycyclic aromatic hydrocarbons in urban environments linked to wintertime wood-burning episodes”. In: *Atmos. Chem. Phys.* 21.23, pp. 17865–17883.

Vehkamäki, Hanna and Ilona Riipinen (2012). “Thermodynamics and kinetics of atmospheric aerosol particle formation and growth”. In: *Chemical Society Reviews* 41.15, pp. 5160–5173.

Vereecken, L. and J. Peeters (2009). “Decomposition of substituted alkoxy radicals—part I: a generalized structure–activity relationship for reaction barrier heights”. In: *Physical Chemistry Chemical Physics* 11.40, pp. 9062–9074.

Vereecken, L. et al. (2021). “Theoretical and experimental study of peroxy and alkoxy radicals in the NO3-initiated oxidation of isoprene”. In: *Physical Chemistry Chemical Physics*.

Veres, P. et al. (2008). “Development of negative-ion proton-transfer chemical-ionization mass spectrometry (NI-PT-CIMS) for the measurement of gas-phase organic acids in the atmosphere”. In: *International Journal of Mass Spectrometry* 274.1-3, pp. 48–55.

Wang, S. et al. (2017). “Formation of Highly Oxidized Radicals and Multifunctional Products from the Atmospheric Oxidation of Alkylbenzenes”. In: *Environ Sci Technol* 51.15, pp. 8442–8449.

Wang, Y. et al. (2019). “The formation of nitro-aromatic compounds under high NOx and anthropogenic VOC conditions in urban Beijing, China”. In: *Atmos. Chem. Phys.* 19.11, pp. 7649–7665.

Wang, Y. et al. (2020). “Oxygenated products formed from OH-initiated reactions of trimethylbenzene: autoxidation and accretion”. In: *Atmos. Chem. Phys.* 20.15, pp. 9563–9579.

Watne, A. K. et al. (2018). “Fresh and Oxidized Emissions from In-Use Transit Buses Running on Diesel, Biodiesel, and CNG”. In: *Environ Sci Technol* 52.14, pp. 7720–7728.

Wennberg, Paul O. et al. (2018). “Gas-Phase Reactions of Isoprene and Its Major Oxidation Products”. In: *Chemical Reviews* 118.7, pp. 3337–3390.

Wildt, J. et al. (2014). “Suppression of new particle formation from monoterpene oxidation by NO_x”. In: *Atmos. Chem. Phys.* 14.6, pp. 2789–2804.

World Health, Organization (2016). *Ambient air pollution: a global assessment of exposure and burden of disease*. Geneva: World Health Organization.

Wu, R. et al. (2021). “Molecular composition and volatility of multi-generation products formed from isoprene oxidation by nitrate radical”. In: *Atmos. Chem. Phys.* 21.13, pp. 10799–10824.

Wyche, K. P. et al. (2009). “Gas phase precursors to anthropogenic secondary organic aerosol: detailed observations of 1,3,5-trimethylbenzene photooxidation”. In: *Atmospheric Chemistry and Physics* 9.2, pp. 635–665.

Xavier, C. et al. (2019). “Aerosol mass yields of selected biogenic volatile organic compounds – a theoretical study with nearly explicit gas-phase chemistry”. In: *Atmos. Chem. Phys.* 19.22, pp. 13741–13758.

Xiong, F. et al. (2016). “Photochemical degradation of isoprene-derived 4,1-nitrooxy enal”. In: *Atmos. Chem. Phys.* 16.9, pp. 5595–5610.

Xu, Z. N. et al. (2021). “Multifunctional Products of Isoprene Oxidation in Polluted Atmosphere and Their Contribution to SOA”. In: *Geophysical Research Letters* 48.1, e2020GL089276.

Yao, L. et al. (2016). “Detection of atmospheric gaseous amines and amides by a high-resolution time-of-flight chemical ionization mass spectrometer with protonated ethanol reagent ions”. In: *Atmos. Chem. Phys.* 16.22, pp. 14527–14543.

Yatavelli, R. L. N. et al. (2012). “A Chemical Ionization High-Resolution Time-of-Flight Mass Spectrometer Coupled to a Micro Orifice Volatilization Impactor (MOVI-HRToF-CIMS) for Analysis of Gas and Particle-Phase Organic Species”. In: *Aerosol Science and Technology* 46.12, pp. 1313–1327.

Ye, C. et al. (2021). “Chemical characterization of oxygenated organic compounds in the gas phase and particle phase using iodide CIMS with FIGAERO in urban air”. In: *Atmos. Chem. Phys.* 21.11, pp. 8455–8478.

Ylisirniö, A. et al. (2021). “On the calibration of FIGAERO-ToF-CIMS: importance and impact of calibrant delivery for the particle-phase calibration”. In: *Atmos. Meas. Tech.* 14.1, pp. 355–367.

Yuan, B. et al. (2016). “A high-resolution time-of-flight chemical ionization mass spectrometer utilizing hydronium ions (H3O+ ToF-CIMS) for measurements of volatile organic compounds in the atmosphere”. In: *Atmos. Meas. Tech.* 9.6, pp. 2735–2752.

Zaytsev, A. et al. (2019). “Using collision-induced dissociation to constrain sensitivity of ammonia chemical ionization mass spectrometry (NH4+ CIMS) to oxygenated volatile organic compounds”. In: *Atmos. Meas. Tech.* 12.3, pp. 1861–1870.

Zha, Q. Z. et al. (2018). “Vertical characterization of highly oxygenated molecules (HOMs) below and above a boreal forest canopy”. In: *Atmospheric Chemistry and Physics* 18.23, pp. 17437–17450.

Zhao, D. et al. (2021). “Highly oxygenated organic molecule (HOM) formation in the isoprene oxidation by NO3 radical”. In: *Atmos. Chem. Phys.* 21.12, pp. 9681–9704.

Zhao, Y., J. A. Thornton, and H. O. T. Pye (2018). “Quantitative constraints on autoxidation and dimer formation from direct probing of monoterpene-derived peroxy radical chemistry”. In: *Proceedings of the National Academy of Sciences of the United States of America* 115.48, pp. 12142–12147.

Ziemann, P. J. and R. Atkinson (2012). “Kinetics, products, and mechanisms of secondary organic aerosol formation”. In: *Chem Soc Rev* 41.19, pp. 6582–605.

Part II

Appended Papers